Search for Strange Pentaquark Production in e^+e^- Annihilations at $\sqrt{s}=10.58$ GeV and in $\Upsilon(4S)$ Decays

The BABAR Collaboration

April 28, 2018

Abstract

We present a preliminary inclusive search for strange pentaquark production in e^+e^- interactions at a center-of-mass energy of 10.58 GeV using 123 fb⁻¹ of data collected with the *BABAR* detector. We look for the states that have been reported previously: the $\Theta^+(1540)$, interpreted as a $udud\bar{s}$ state; and the $\Xi^{--}(1860)$ and $\Xi^0(1860)$, candidate $dsds\bar{u}$ and $uss(u\bar{u}+d\bar{d})$ states, respectively. In addition we search for other members of the antidecuplet and corresponding octet to which these states are thought to belong. We find no evidence for the production of such states and set preliminary limits on their production cross sections as functions of c.m. momentum. The corresponding limits on the $\Theta^+(1540)$ and $\Xi^{--}(1860)$ rates per $e^+e^- \to q\bar{q}$ event are well below the rates measured for ordinary baryons of similar mass.

Submitted to the $32^{\rm nd}$ International Conference on High-Energy Physics, ICHEP 04, 16 August—22 August 2004, Beijing, China

Stanford Linear Accelerator Center, Stanford University, Stanford, CA 94309

Work supported in part by Department of Energy contract DE-AC03-76SF00515.

The BABAR Collaboration,

B. Aubert, R. Barate, D. Boutigny, F. Couderc, J.-M. Gaillard, A. Hicheur, Y. Karyotakis, J. P. Lees, V. Tisserand, A. Zghiche

Laboratoire de Physique des Particules, F-74941 Annecy-le-Vieux, France

A. Palano, A. Pompili

Università di Bari, Dipartimento di Fisica and INFN, I-70126 Bari, Italy

J. C. Chen, N. D. Qi, G. Rong, P. Wang, Y. S. Zhu Institute of High Energy Physics, Beijing 100039, China

G. Eigen, I. Ofte, B. Stugu

University of Bergen, Inst. of Physics, N-5007 Bergen, Norway

G. S. Abrams, A. W. Borgland, A. B. Breon, D. N. Brown, J. Button-Shafer, R. N. Cahn, E. Charles, C. T. Day, M. S. Gill, A. V. Gritsan, Y. Groysman, R. G. Jacobsen, R. W. Kadel, J. Kadyk, L. T. Kerth, Yu. G. Kolomensky, G. Kukartsev, G. Lynch, L. M. Mir, P. J. Oddone, T. J. Orimoto, M. Pripstein, N. A. Roe, M. T. Ronan, V. G. Shelkov, W. A. Wenzel

Lawrence Berkeley National Laboratory and University of California, Berkeley, CA 94720, USA

- M. Barrett, K. E. Ford, T. J. Harrison, A. J. Hart, C. M. Hawkes, S. E. Morgan, A. T. Watson University of Birmingham, Birmingham, B15 2TT, United Kingdom
 - M. Fritsch, K. Goetzen, T. Held, H. Koch, B. Lewandowski, M. Pelizaeus, M. Steinke Ruhr Universität Bochum, Institut für Experimentalphysik 1, D-44780 Bochum, Germany
 - J. T. Boyd, N. Chevalier, W. N. Cottingham, M. P. Kelly, T. E. Latham, F. F. Wilson University of Bristol, Bristol BS8 1TL, United Kingdom
- T. Cuhadar-Donszelmann, C. Hearty, N. S. Knecht, T. S. Mattison, J. A. McKenna, D. Thiessen University of British Columbia, Vancouver, BC, Canada V6T 1Z1

A. Khan, P. Kyberd, L. Teodorescu

Brunel University, Uxbridge, Middlesex UB8 3PH, United Kingdom

A. E. Blinov, V. E. Blinov, V. P. Druzhinin, V. B. Golubev, V. N. Ivanchenko, E. A. Kravchenko, A. P. Onuchin, S. I. Serednyakov, Yu. I. Skovpen, E. P. Solodov, A. N. Yushkov Budker Institute of Nuclear Physics, Novosibirsk 630090, Russia

D. Best, M. Bruinsma, M. Chao, I. Eschrich, D. Kirkby, A. J. Lankford, M. Mandelkern, R. K. Mommsen, W. Roethel, D. P. Stoker

University of California at Irvine, Irvine, CA 92697, USA

C. Buchanan, B. L. Hartfiel

University of California at Los Angeles, Los Angeles, CA 90024, USA

S. D. Foulkes, J. W. Gary, B. C. Shen, K. Wang University of California at Riverside, Riverside, CA 92521, USA

- D. del Re, H. K. Hadavand, E. J. Hill, D. B. MacFarlane, H. P. Paar, Sh. Rahatlou, V. Sharma University of California at San Diego, La Jolla, CA 92093, USA
- J. W. Berryhill, C. Campagnari, B. Dahmes, O. Long, A. Lu, M. A. Mazur, J. D. Richman, W. Verkerke University of California at Santa Barbara, Santa Barbara, CA 93106, USA
 - T. W. Beck, A. M. Eisner, C. A. Heusch, J. Kroseberg, W. S. Lockman, G. Nesom, T. Schalk, B. A. Schumm, A. Seiden, P. Spradlin, D. C. Williams, M. G. Wilson
 - University of California at Santa Cruz, Institute for Particle Physics, Santa Cruz, CA 95064, USA
 - J. Albert, E. Chen, G. P. Dubois-Felsmann, A. Dvoretskii, D. G. Hitlin, I. Narsky, T. Piatenko, F. C. Porter, A. Ryd, A. Samuel, S. Yang

California Institute of Technology, Pasadena, CA 91125, USA

- S. Jayatilleke, G. Mancinelli, B. T. Meadows, M. D. Sokoloff University of Cincinnati, Cincinnati, OH 45221, USA
- T. Abe, F. Blanc, P. Bloom, S. Chen, W. T. Ford, U. Nauenberg, A. Olivas, P. Rankin, J. G. Smith, J. Zhang, L. Zhang

University of Colorado, Boulder, CO 80309, USA

- A. Chen, J. L. Harton, A. Soffer, W. H. Toki, R. J. Wilson, Q. Zeng Colorado State University, Fort Collins, CO 80523, USA
- D. Altenburg, T. Brandt, J. Brose, M. Dickopp, E. Feltresi, A. Hauke, H. M. Lacker, R. Müller-Pfefferkorn, R. Nogowski, S. Otto, A. Petzold, J. Schubert, K. R. Schubert, R. Schwierz, B. Spaan, J. E. Sundermann Technische Universität Dresden, Institut für Kern- und Teilchenphysik, D-01062 Dresden, Germany
- D. Bernard, G. R. Bonneaud, F. Brochard, P. Grenier, S. Schrenk, Ch. Thiebaux, G. Vasileiadis, M. Verderi Ecole Polytechnique, LLR, F-91128 Palaiseau, France
 - D. J. Bard, P. J. Clark, D. Lavin, F. Muheim, S. Playfer, Y. Xie University of Edinburgh, Edinburgh EH9 3JZ, United Kingdom
 - M. Andreotti, V. Azzolini, D. Bettoni, C. Bozzi, R. Calabrese, G. Cibinetto, E. Luppi, M. Negrini, L. Piemontese, A. Sarti

Università di Ferrara, Dipartimento di Fisica and INFN, I-44100 Ferrara, Italy

E. Treadwell

Florida A&M University, Tallahassee, FL 32307, USA

F. Anulli, R. Baldini-Ferroli, A. Calcaterra, R. de Sangro, G. Finocchiaro, P. Patteri, I. M. Peruzzi, M. Piccolo, A. Zallo

Laboratori Nazionali di Frascati dell'INFN, I-00044 Frascati, Italy

A. Buzzo, R. Capra, R. Contri, G. Crosetti, M. Lo Vetere, M. Macri, M. R. Monge, S. Passaggio, C. Patrignani, E. Robutti, A. Santroni, S. Tosi

Università di Genova, Dipartimento di Fisica and INFN, I-16146 Genova, Italy

S. Bailey, G. Brandenburg, K. S. Chaisanguanthum, M. Morii, E. Won Harvard University, Cambridge, MA 02138, USA R. S. Dubitzky, U. Langenegger

Universität Heidelberg, Physikalisches Institut, Philosophenweg 12, D-69120 Heidelberg, Germany

W. Bhimji, D. A. Bowerman, P. D. Dauncey, U. Egede, J. R. Gaillard, G. W. Morton, J. A. Nash, M. B. Nikolich, G. P. Taylor

Imperial College London, London, SW7 2AZ, United Kingdom

M. J. Charles, G. J. Grenier, U. Mallik University of Iowa, Iowa City, IA 52242, USA

J. Cochran, H. B. Crawley, J. Lamsa, W. T. Meyer, S. Prell, E. I. Rosenberg, A. E. Rubin, J. Yi Iowa State University, Ames, IA 50011-3160, USA

M. Biasini, R. Covarelli, M. Pioppi

Università di Perugia, Dipartimento di Fisica and INFN, I-06100 Perugia, Italy

M. Davier, X. Giroux, G. Grosdidier, A. Höcker, S. Laplace, F. Le Diberder, V. Lepeltier, A. M. Lutz, T. C. Petersen, S. Plaszczynski, M. H. Schune, L. Tantot, G. Wormser

Laboratoire de l'Accélérateur Linéaire, F-91898 Orsay, France

C. H. Cheng, D. J. Lange, M. C. Simani, D. M. Wright Lawrence Livermore National Laboratory, Livermore, CA 94550, USA

- A. J. Bevan, C. A. Chavez, J. P. Coleman, I. J. Forster, J. R. Fry, E. Gabathuler, R. Gamet, D. E. Hutchcroft, R. J. Parry, D. J. Payne, R. J. Sloane, C. Touramanis University of Liverpool, Liverpool L69 72E, United Kingdom
 - J. J. Back, ¹ C. M. Cormack, P. F. Harrison, ¹ F. Di Lodovico, G. B. Mohanty ¹

 Queen Mary, University of London, E1 4NS, United Kingdom
- C. L. Brown, G. Cowan, R. L. Flack, H. U. Flaecher, M. G. Green, P. S. Jackson, T. R. McMahon, S. Ricciardi, F. Salvatore, M. A. Winter

University of London, Royal Holloway and Bedford New College, Egham, Surrey TW20 0EX, United Kingdom

D. Brown, C. L. Davis

University of Louisville, Louisville, KY 40292, USA

J. Allison, N. R. Barlow, R. J. Barlow, P. A. Hart, M. C. Hodgkinson, G. D. Lafferty, A. J. Lyon, J. C. Williams

University of Manchester, Manchester M13 9PL, United Kingdom

- A. Farbin, W. D. Hulsbergen, A. Jawahery, D. Kovalskyi, C. K. Lae, V. Lillard, D. A. Roberts University of Maryland, College Park, MD 20742, USA
- G. Blaylock, C. Dallapiccola, K. T. Flood, S. S. Hertzbach, R. Kofler, V. B. Koptchev, T. B. Moore, S. Saremi, H. Staengle, S. Willocq

University of Massachusetts, Amherst, MA 01003, USA

¹Now at Department of Physics, University of Warwick, Coventry, United Kingdom

R. Cowan, G. Sciolla, S. J. Sekula, F. Taylor, R. K. Yamamoto

Massachusetts Institute of Technology, Laboratory for Nuclear Science, Cambridge, MA 02139, USA

D. J. J. Mangeol, P. M. Patel, S. H. Robertson

McGill University, Montréal, QC, Canada H3A 2T8

A. Lazzaro, V. Lombardo, F. Palombo

Università di Milano, Dipartimento di Fisica and INFN, I-20133 Milano, Italy

J. M. Bauer, L. Cremaldi, V. Eschenburg, R. Godang, R. Kroeger, J. Reidy, D. A. Sanders, D. J. Summers, H. W. Zhao

University of Mississippi, University, MS 38677, USA

S. Brunet, D. Côté, P. Taras

Université de Montréal, Laboratoire René J. A. Lévesque, Montréal, QC, Canada H3C 3J7

H. Nicholson

Mount Holyoke College, South Hadley, MA 01075, USA

N. Cavallo,² F. Fabozzi,² C. Gatto, L. Lista, D. Monorchio, P. Paolucci, D. Piccolo, C. Sciacca Università di Napoli Federico II, Dipartimento di Scienze Fisiche and INFN, I-80126, Napoli, Italy

M. Baak, H. Bulten, G. Raven, H. L. Snoek, L. Wilden

NIKHEF, National Institute for Nuclear Physics and High Energy Physics, NL-1009 DB Amsterdam, The Netherlands

C. P. Jessop, J. M. LoSecco

University of Notre Dame, Notre Dame, IN 46556, USA

T. Allmendinger, K. K. Gan, K. Honscheid, D. Hufnagel, H. Kagan, R. Kass, T. Pulliam, A. M. Rahimi, R. Ter-Antonyan, Q. K. Wong

Ohio State University, Columbus, OH 43210, USA

J. Brau, R. Frey, O. Igonkina, C. T. Potter, N. B. Sinev, D. Strom, E. Torrence University of Oregon, Eugene, OR 97403, USA

F. Colecchia, A. Dorigo, F. Galeazzi, M. Margoni, M. Morandin, M. Posocco, M. Rotondo, F. Simonetto, R. Stroili, G. Tiozzo, C. Voci

Università di Padova, Dipartimento di Fisica and INFN, I-35131 Padova, Italy

M. Benayoun, H. Briand, J. Chauveau, P. David, Ch. de la Vaissière, L. Del Buono, O. Hamon, M. J. John, Ph. Leruste, J. Malcles, J. Ocariz, M. Pivk, L. Roos, S. T'Jampens, G. Therin

Universités Paris VI et VII, Laboratoire de Physique Nucléaire et de Hautes Energies, F-75252 Paris, France

P. F. Manfredi, V. Re

Università di Pavia, Dipartimento di Elettronica and INFN, I-27100 Pavia, Italy

²Also with Università della Basilicata, Potenza, Italy

P. K. Behera, L. Gladney, Q. H. Guo, J. Panetta University of Pennsylvania, Philadelphia, PA 19104, USA

C. Angelini, G. Batignani, S. Bettarini, M. Bondioli, F. Bucci, G. Calderini, M. Carpinelli, F. Forti, M. A. Giorgi, A. Lusiani, G. Marchiori, F. Martinez-Vidal, M. Morganti, N. Neri, E. Paoloni, M. Rama, G. Rizzo, F. Sandrelli, J. Walsh

Università di Pisa, Dipartimento di Fisica, Scuola Normale Superiore and INFN, I-56127 Pisa, Italy

M. Haire, D. Judd, K. Paick, D. E. Wagoner

Prairie View A&M University, Prairie View, TX 77446, USA

- N. Danielson, P. Elmer, Y. P. Lau, C. Lu, V. Miftakov, J. Olsen, A. J. S. Smith, A. V. Telnov Princeton University, Princeton, NJ 08544, USA
- F. Bellini, G. Cavoto, R. Faccini, F. Ferrarotto, F. Ferroni, M. Gaspero, L. Li Gioi, M. A. Mazzoni, S. Morganti, M. Pierini, G. Piredda, F. Safai Tehrani, C. Voena

Università di Roma La Sapienza, Dipartimento di Fisica and INFN, I-00185 Roma, Italy

S. Christ, G. Wagner, R. Waldi Universität Rostock, D-18051 Rostock, Germany

T. Adye, N. De Groot, B. Franck, N. I. Geddes, G. P. Gopal, E. O. Olaiya Rutherford Appleton Laboratory, Chilton, Didcot, Oxon, OX11 0QX, United Kingdom

R. Aleksan, S. Emery, A. Gaidot, S. F. Ganzhur, P.-F. Giraud, G. Hamel de Monchenault, W. Kozanecki, M. Legendre, G. W. London, B. Mayer, G. Schott, G. Vasseur, Ch. Yèche, M. Zito DSM/Dapnia, CEA/Saclay, F-91191 Gif-sur-Yvette, France

> M. V. Purohit, A. W. Weidemann, J. R. Wilson, F. X. Yumiceva University of South Carolina, Columbia, SC 29208, USA

D. Aston, R. Bartoldus, N. Berger, A. M. Boyarski, O. L. Buchmueller, R. Claus, M. R. Convery, M. Cristinziani, G. De Nardo, D. Dong, J. Dorfan, D. Dujmic, W. Dunwoodie, E. E. Elsen, S. Fan, R. C. Field, T. Glanzman, S. J. Gowdy, T. Hadig, V. Halyo, C. Hast, T. Hryn'ova, W. R. Innes, M. H. Kelsey, P. Kim, M. L. Kocian, D. W. G. S. Leith, J. Libby, S. Luitz, V. Luth, H. L. Lynch, H. Marsiske, R. Messner, D. R. Muller, C. P. O'Grady, V. E. Ozcan, A. Perazzo, M. Perl, S. Petrak, B. N. Ratcliff, A. Roodman, A. A. Salnikov, R. H. Schindler, J. Schwiening, G. Simi, A. Snyder, A. Soha, J. Stelzer, D. Su, M. K. Sullivan, J. Va'vra, S. R. Wagner, M. Weaver, A. J. R. Weinstein, W. J. Wisniewski, M. Wittgen, D. H. Wright, A. K. Yarritu, C. C. Young
Stanford Linear Accelerator Center, Stanford, CA 94309, USA

P. R. Burchat, A. J. Edwards, T. I. Meyer, B. A. Petersen, C. Roat Stanford University, Stanford, CA 94305-4060, USA

S. Ahmed, M. S. Alam, J. A. Ernst, M. A. Saeed, M. Saleem, F. R. Wappler State University of New York, Albany, NY 12222, USA

³Also with IFIC, Instituto de Física Corpuscular, CSIC-Universidad de Valencia, Valencia, Spain
⁴Also with Princeton University, Princeton, USA

W. Bugg, M. Krishnamurthy, S. M. Spanier University of Tennessee, Knoxville, TN 37996, USA

R. Eckmann, H. Kim, J. L. Ritchie, A. Satpathy, R. F. Schwitters University of Texas at Austin, Austin, TX 78712, USA

J. M. Izen, I. Kitayama, X. C. Lou, S. Ye University of Texas at Dallas, Richardson, TX 75083, USA

F. Bianchi, M. Bona, F. Gallo, D. Gamba

Università di Torino, Dipartimento di Fisica Sperimentale and INFN, I-10125 Torino, Italy

L. Bosisio, C. Cartaro, F. Cossutti, G. Della Ricca, S. Dittongo, S. Grancagnolo, L. Lanceri, P. Poropat,⁵
L. Vitale, G. Vuagnin

Università di Trieste, Dipartimento di Fisica and INFN, I-34127 Trieste, Italy

R. S. Panvini

Vanderbilt University, Nashville, TN 37235, USA

Sw. Banerjee, C. M. Brown, D. Fortin, P. D. Jackson, R. Kowalewski, J. M. Roney, R. J. Sobie University of Victoria, Victoria, BC, Canada V8W 3P6

H. R. Band, B. Cheng, S. Dasu, M. Datta, A. M. Eichenbaum, M. Graham, J. J. Hollar, J. R. Johnson, P. E. Kutter, H. Li, R. Liu, A. Mihalyi, A. K. Mohapatra, Y. Pan, R. Prepost, P. Tan, J. H. von Wimmersperg-Toeller, J. Wu, S. L. Wu, Z. Yu

University of Wisconsin, Madison, WI 53706, USA

M. G. Greene, H. Neal

Yale University, New Haven, CT 06511, USA

 $^{^5}$ Deceased

1 Introduction

Recently several experimental groups have reported observations of a new, manifestly exotic (B=1, S=1) baryon resonance, called the $\Theta^+(1540)$ [1]-[7], with an unusually narrow width (Γ <8 MeV/ c^2) for a particle in this mass range that has open channels to strong decay. Also, the NA49 experiment reported evidence for an additional narrow exotic (B=1, Q=S=-2) state, called Ξ^{--} , as well as corresponding Ξ^0 state, with masses close to 1862 MeV/ c^2 [8]. More recently the H1 collaboration reported a narrow (Γ < 30 MeV/ c^2) exotic charmed (B=1, C=-1) resonance, Θ_c^0 , with a mass of 3099 MeV/ c^2 . The simplest quark assignments consistent with the quantum numbers of Θ^+ , Ξ^{--} and Θ_c^0 are $(udud\bar{s})$, $(dsds\bar{u})$ and $(udud\bar{c})$, respectively; therefore these observed states are regarded as pentaquark candidates.

These results have prompted a surge of pentaquark searches in experimental data of many kinds, mostly with negative results [10]. Several theoretical models [11, 12, 13] have been proposed to describe possible pentaquark structure. They predict that the lowest mass states containing u,d and s quarks should occupy a spin-1/2 antidecuplet and octet, as illustrated in Fig. 1. Predictions for the masses of the unobserved N and Σ states vary; M_N might be anywhere between ~ 150 MeV/ c^2 below M_{Θ} and $\sim M_{\Xi}$, and M_{Σ} anywhere between $\sim M_{\Theta}$ and ~ 150 MeV/ c^2 above M_{Ξ} . In order to distinguish pentaquarks from ordinary baryons, we adopt a notation that has names corresponding to ordinary baryons with similar s quark content, plus a subscript 5. For example, the Ξ_5^- pentaquark $(dss(u\bar{u}+d\bar{d}))$ corresponds to the ordinary Ξ^- (dss) baryon.

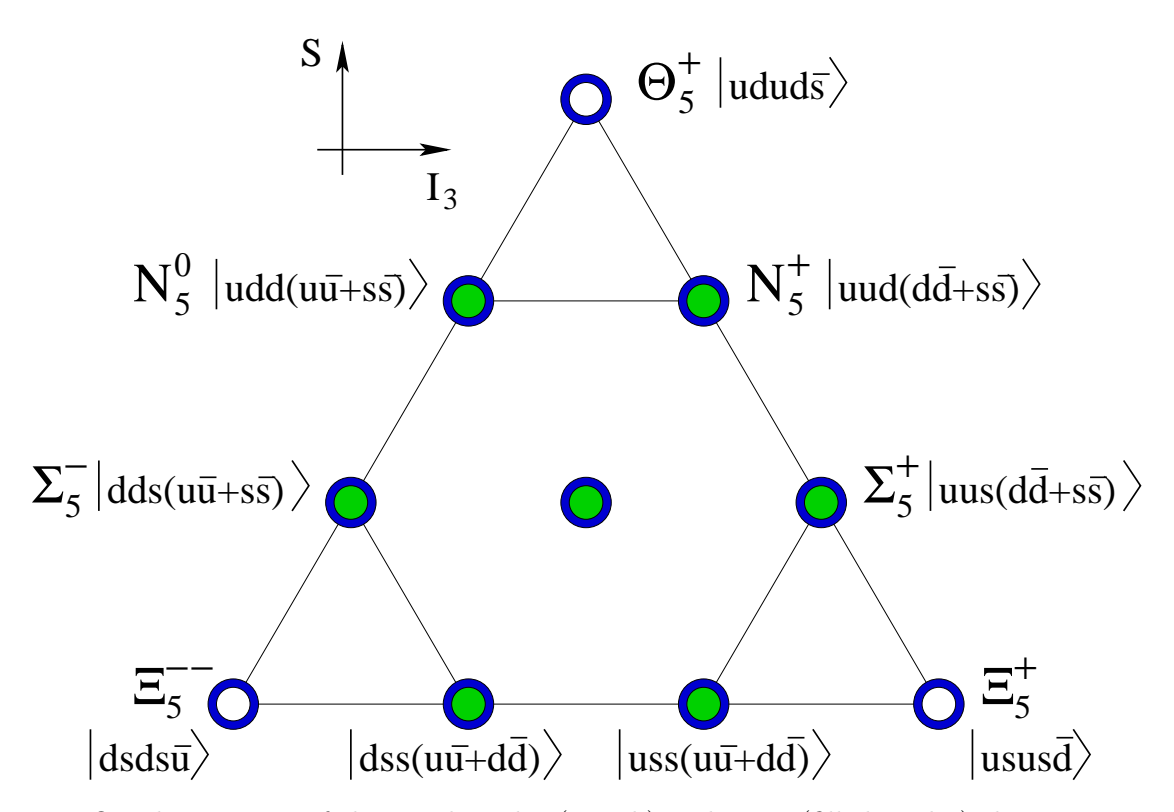


Figure 1: Quark structure of the antidecuplet (annuli) and octet (filled circles) that are generally assumed for the lowest-mass pentaquarks. Strangeness increases in the vertical direction and the third component of isospin in the horizontal.

Although experiments with a baryon in the beam or the target might have some advantage in pentaquark production, e^+e^- interactions are also known for democratic production of hadrons. Baryons with nonzero beauty, charm, strangeness (up to three units) and/or orbital angular momentum have been observed with production rates that appear to depend on the mass and spin, but not quark content. If pentaquarks are produced similarly, then one might expect a pentaquark rate as high as that for an ordinary baryon of the same mass and spin, i.e. about $8 \times 10^{-4} \ \Theta_5^+$ and about $4 \times 10^{-5} \ \Xi_5^{--}$ per $e^+e^- \to$ hadrons event at $\sqrt{s} = 10.58$ GeV [15]. Decays of B mesons are also known to produce a rather high rate of baryons and so provide another fertile hunting ground. In both cases we expect any set of pentaquark states forming a multiplet of approximately equal mass to be produced at roughly equal rates, so that access to all narrow states is available.

Here we describe a program of inclusive searches for the reported states and also the other members of the hypothetical antidecuplet and octet in data from the *BABAR* experiment, which include both $e^+e^- \to q\bar{q}$, q=udsc, events and the production of $\Upsilon(4S)$ mesons, which decay into $B\bar{B}$ pairs. We have concentrated on decay modes involving strange particles and protons, which are easily reconstructed in our detector. All states except the N_5 have nonzero strangeness, and the N_5 and Σ_5 have hidden strangeness divided in some way between the octet and antidecuplet states. Since the production mechanism, and hence the momentum spectra, for pentaquarks is unknown, we consider differential production cross sections $d\sigma/dp^*$ per unit momentum p^* in the e^+e^- center-of-mass (c.m.) frame, which are to first order independent of any model, and applicable to the sum of all production processes at $\sqrt{s}=10.58$ GeV. After describing some common aspects of the analyses in section 2, we describe searches in three classes of decay modes in the next three sections. Upper limits on pentaquark production are discussed in section 6, and we summarize the results in section 7.

2 Data and Simulation

The data sample used in the analysis comprises the runs of the BABAR experiment through 2003, and amounts to an integrated luminosity of $123\,\mathrm{fb}^{-1}$, roughly 90% (10%) of which was recorded on (below) the $\Upsilon(4S)$ resonance at a c.m. energy of $\sqrt{s}=10.58$ (10.54) GeV. The BABAR detector is described in detail in Ref. [14]. Here we use charged tracks reconstructed in the 5-layer silicon vertex detector (SVT) and the 40-layer drift chamber (DCH), and identified using a combination of energy loss measured in these two subdetectors and Cherenkov angles measured in the detector of internally reflected Cherenkov radiation (DIRC). The charged particle momentum resolution is given by $(\delta p_T/p_T)^2 = (0.0013p_T)^2 + 0.0045^2$, where p_T is the momentum transverse to the beam axis in GeV/c. Loose particle identification is required on most particles, giving in each case nearly 100% efficiency with a sizable background reduction. Tighter requirements are made where noted, giving identification efficiencies ranging from 80–99% and background rejection factors of 12–100. Photons are detected by a CsI(Tl) electromagnetic calorimeter (EMC) with an energy resolution of $\sigma(E)/E = 0.023 \cdot (E/GeV)^{-1/4} \oplus 0.019$. Our invariant mass resolution for a given decay mode is better than that of any experiment reporting the observation of a pentaquark candidate with that mode available.

Minimal hadronic event selection is performed, as we wish to be as inclusive as possible and maintain maximum signal efficiency. We simply require three reconstructed charged tracks in the event. The vast majority of the events are hadronic; lepton-pair events are expected to contribute negligible background in the signal regions; two-photon events and events with a hard initial-state photon contribute only at low momenta. The acceptance for a pentaquark signal from any of these

sources is well understood; if a signal is found, we can attempt to isolate the source with cuts on the event properties.

Samples of simulated $e^+e^- \to q\bar{q}$, where q=udsc, are generated using the JETSET [16] Monte Carlo generator combined with a detailed simulation of the BABAR detector, in order to study backgrounds and "control" particles – known resonances with similar masses and decay modes to the pentaquark in question. By comparing with the same particles reconstructed in the data, we verify the simulation of the invariant mass resolutions and biases of the detector, an essential ingredient in the evaluation of any new signal, or limit where no signal is seen.

In order to evaluate pentaquark reconstruction efficiencies, we simulate pentaquark signals within our standard software with special parameter settings of the JETSET generator. For each pentaquark state we take an existing baryon as a stand-in, change its mass and width to match the desired pentaquark properties, and force a particular decay mode, with all other JETSET parameters left unchanged. The generator thus gives the stand-in particles a momentum spectrum based on the pentaquark mass, but the stand-in flavor. We make no attempt here to conserve flavor in the production process, as we are only concerned with providing an appropriate number and distribution of additional particles in the event. We do not know the production mechanism for such five-quark states; however, to make the measurement we only need the efficiency as a function of the relevant variables, in this case momentum and polar angle in the laboratory frame, so any smooth distribution that covers the entire range of these variables is sufficient. Effects such as the type, multiplicity and proximity of other particles in the event can be studied by using different stand-in baryons; such effects are found to be smaller than the other systematic uncertainties. The stand-in particles used to generate our signal samples are summarized in Table 1.

Table 1: Baryons used in the simulation to generate pentaguark signal samples.

Pentaquark	Existing	Mass	Width	# of
Signal mode	Baryon Used	(MeV/c^2)	(MeV/c^2)	Events
$\Theta_5^+ \longrightarrow pK_S^0$	Δ^+	1540	1	120,000
$\Xi_5^{}$ $\rightarrow \Xi^-\pi^-$	Δ^{++}	1862	1	120,000
	Σ_c^{++}	1862	1	98,000
$\Xi_5^0 \longrightarrow \Xi^-\pi^+$	= *0	1862	1	60,000
$\Sigma_5^0 \longrightarrow \Xi^- K^+$	<u>=</u> *0	1862	1	120,000
$\Xi_5^- \longrightarrow \Lambda^0 K^-$	<u>=</u> *-	1862	1	29,000
$\Xi_5^+/N_5^+ \to \Lambda^0 K^+$	<u>=</u> *+	1862	1	29,000
$\Xi_5^0 \longrightarrow \Lambda^0 K_{\scriptscriptstyle S}^0$	= *0	1862	1	29,000
$\Xi_5^- \longrightarrow \Sigma^0 K^-$	<u>=</u> *-	1862	1	27,000
$\Xi_5^+/N_5^+ \to \Sigma^0 K^+$	<u>=</u> *+	1862	1	27,000
$\Xi_5^0 \longrightarrow \Sigma^0 K_s^0$	= *0	1862	1	25,000

3 Search for the $\Theta_5^+(1540) \to pK_s^0$

We reconstruct Θ_5^+ candidates in the pK_S^0 decay mode, where $K_S^0 \to \pi^-\pi^+$, with selection criteria designed for high efficiency and low bias against any production mechanism. A sample of K_S^0 candidates is obtained from all pairs of oppositely charged tracks passing loose pion identification requirements that pass within 6 mm of each other. Each pair is required to: have a total momentum vector extrapolating within 6 mm (32 mm) of the interaction point (IP) in the plane transverse to (along) the beam direction; have a positive flight distance, defined as the projection on the candidate momentum direction of a vector from its point of closest approach to the beam axis to its decay point; and have an invariant mass within 10 MeV/ c^2 of the nominal K_S^0 mass. We also require the helicity angle θ_H of the candidate, defined as the angle between the π^+ and the reconstructed $\pi^+\pi^-$ flight direction in the $\pi^+\pi^-$ rest frame, to satisfy $|\cos\theta_H| < 0.8$, eliminating background from Λ^0 decays and photon conversions and reducing combinatoric background.

We combine the surviving K_s^0 candidates with identified p and \bar{p} tracks that extrapolate within 15 mm (10 cm) of the IP in the plane transverse to (along) the beam direction. The simulated signal reconstruction efficiency varies with p^* , the pK_s^0 momentum in the e^+e^- c.m. frame, from 13% at low p^* to 22% at high p^* . The invariant mass distribution of these pairs is shown in Fig. 2. There is a clear peak at 2285 MeV/ c^2 from $\Lambda_c^+ \to pK_s^0$ but no other sharp structure. The Λ_c^+ peak (upper right plot) shows a mass resolution of better than 6 MeV/ c^2 and contains roughly 52,000 entries, demonstrating our sensitivity to the presence of a narrow resonance. The lower plots zoom in on the mass ranges 1400–1600 and 1600–1800 MeV/ c^2 . The Θ_5^+ has been reported at values between 1520 and 1540 MeV/ c^2 . There is no enhancement in our data anywhere in this region. The pK_s^0 decay mode is also possible for the Σ_5^+ states, whose masses might be expected to be between that of the Θ_5^+ and about 2000 MeV/ c^2 depending on their strange quark content. There is no sign of a narrow resonance anywhere in this region.

We consider several additional criteria that might enhance a pentaquark signal. More stringent requirements on the flight distance of the K_s^0 candidate give a much cleaner K_s^0 sample at the expense of efficiency at low momentum. This enhances the Λ_c^+ signal to noise, but does not reveal any additional structure. If a pentaguark is produced in an $e^+e^$ annihilation event, then there must also be an antibaryon (or anti-pentaquark) in the event, among whose decay products is either an antiproton or antineutron. In the case of the Θ_5^+ decaying to pK_s^0 , the K_s^0 must have been a K^0 rather than a \bar{K}^0 , and there must be a compensating particle in the event with strangeness -1, which might often be a K^- . We consider all subsets of the pK_s^0 combinations for which there is also at least one loosely identified K^- and/or \bar{p} track in the event. In all cases the data quantity is reduced, the Λ_c^+ signal is still visible and there is no sign of a pentaquark peak. Following work by the CLAS and NA49 experiments [3, 8], we reconstruct a possible $N^*(2400) \to K^- K_s^0 p$ using the selected pK_s^0 pairs and an additional loosely identified K^- candidate. We observe no N^* peak in our data. Considering various $K^-K_S^0p$ mass ranges, the pK_S^0 mass distribution for $K^-K_s^0p$ masses near 2400 MeV/ c^2 shows no pentaquark signal, and is indistinguishable from the pK_s^0 mass distributions in nearby $K^-K_s^0p$ mass ranges. Requiring in addition a recoil antiproton yields similar results.

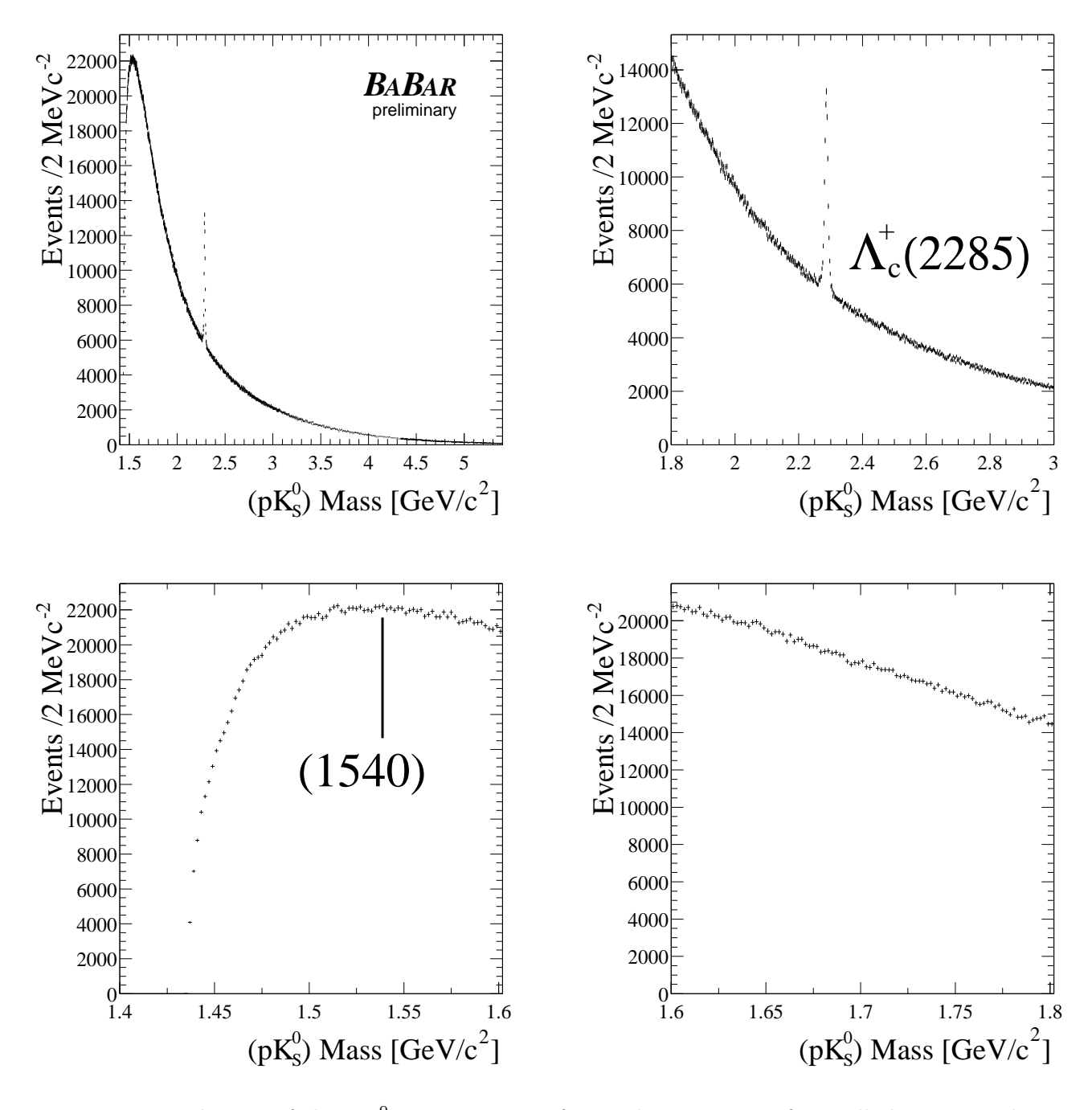


Figure 2: Distribution of the pK_S^0 invariant mass for combinations satisfying all the criteria described in the text. The same data are plotted four times in different pK_S^0 mass regions.

In each of the above cases we split the data into ten bins of p^* , in order to enhance our sensitivity to any production mechanism that gives a momentum spectrum different from that of our background. The bins are 500 MeV/ c^2 wide and cover the p^* range from zero to 5 GeV/ c^2 , the kinematic limit for a particle of mass 1700 MeV/ c^2 . The background is much smaller at higher p^* , so we are more sensitive to mechanisms that produce harder spectra. In no case is there any sign of a pentaquark signal.

We quantify these null results for the Θ_5^+ , assuming a mass of 1540 MeV/ c^2 . In order to reduce model dependence, we consider the ten p^* bins noted above and fit a signal plus background function to the pK_s^0 invariant mass distribution in each bin. The natural width of the Θ_5^+ has not been measured; the best upper limit, $\Gamma < 8 \text{ MeV}/c^2$, is larger than our detector resolution, so we must consider the range of widths up to this value. We use a P-wave Breit-Wigner lineshape multiplied by a phase-space factor and convolved with a resolution function derived from the A_c^+ data and simulation. The latter is a sum of two Gaussian distributions with a common center and an overall rms ranging from 2.5 MeV/ c^2 at low p^* to 1.8 MeV/ c^2 at high p^* ; this is narrower than for the A_c^+ due to the proximity of the Θ_5^+ (1540) to threshold. For the natural width we consider two possibilities, 1 MeV/ c^2 and 8 MeV/ c^2 , corresponding to a very narrow state and the upper limit, respectively. The fits are performed over a wide range, from threshold to 1800 MeV/ c^2 , and the background function is a seventh-order polynomial times a threshold factor.

For the case of our nominal selection criteria (Fig. 2), we obtain the signal yields shown in Fig. 3. In all p^* bins the fit quality is good and the signal is consistent with zero. There is no positive trend in the data, and the roughly symmetric scatter of the points about zero indicates low momentum-dependent bias in the background function. We consider systematic effects in the fitting procedure by varying the signal and background functions and fit range; changes in the fitted signal are negligible compared with the statistical uncertainties. Other selection criteria yield similar results. Since the nominal selection gives the smallest absolute uncertainties after efficiency corrections, we use it to set upper limits on the production cross section in section 6. Varying the mass assumed for the Θ_5^+ has effects consistent with statistics; in no case do we observe a signal, and the uncertainties shown in Fig. 3 are typical.

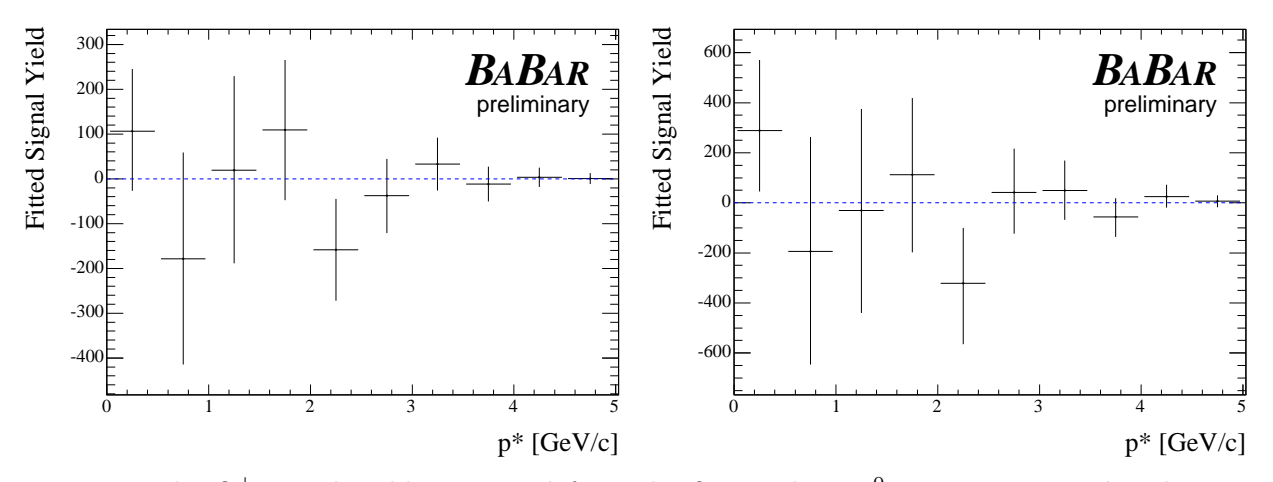


Figure 3: The Θ_5^+ signal yields extracted from the fits to the pK_S^0 invariant mass distributions, assuming a Θ_5^+ mass of 1540 MeV/ c^2 and width $\Gamma=1$ MeV/ c^2 (left) and $\Gamma=8$ MeV/ c^2 (right).

4 Search for $\Xi_5^{--} \to \Xi^- \pi^-$ and $\Xi_5^0 \to \Xi^- \pi^+$

We next search for pentaquark states decaying into a Ξ^- and a charged pion, where $\Xi^- \to$ $\Lambda^0\pi^-$ and $\Lambda^0\to p\pi^-$, including the reported $\Xi_5^{--}(1862)$ and $\Xi_5^0(1862)$. We first reconstruct $\Lambda^0 \to p\pi^-$ candidates from all pairs of charged tracks satisfying loose proton and pion requirements. Efficient and unbiased selection criteria are again applied: the tracks must pass within 6 mm of each other; the candidate have a positive flight distance from the IP; and it must have an invariant mass within 10 MeV/ c^2 of the nominal Λ^0 mass. These candidates are combined with an additional negatively charged track passing loose pion identification requirements to form Ξ^- candidates. These candidates are required to form a good vertex, to have a positive flight distance from the IP, and to have an invariant mass within 20 MeV/ c^2 of the nominal Ξ^- mass. Furthermore the flight distance of the Λ^0 candidate from the $\Lambda^0\pi^$ vertex must be positive. Finally, we combine the Ξ^- candidates with an additional charged track consistent with coming from the IP and passing loose pion identification requirements. The cosine of the angle between the reconstructed Ξ^- trajectory, extrapolated back to the IP, and the additional track is required to be less than 0.998. This last cut is especially important, since the Ξ^- is charged and has a long lifetime; if it has a long flight distance, it can produce a reconstructed track that, if combined with itself, forms a false peak in the invariant mass distribution. The simulated signal reconstruction efficiency varies from 6.5% at low p^* to 12% at high p^* .

The invariant mass distributions for $\Xi^-\pi^-$ and $\Xi^-\pi^+$ are shown in Figs. 4 and 5, respectively. In Fig. 5 there are clear peaks as expected for the $\Xi^{*0}(1530)$ and $\Xi_c^0(2470)$ baryons, but no other structure is visible. In Fig. 4 there is no visible sharp structure at all.

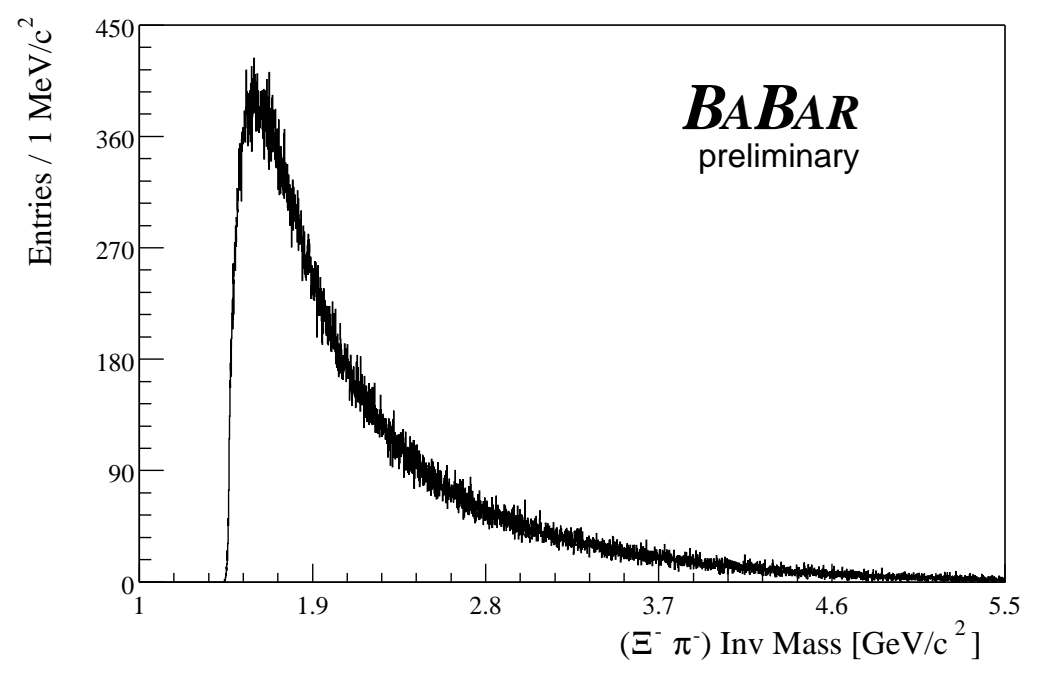


Figure 4: $\Xi^-\pi^-$ invariant mass distribution.

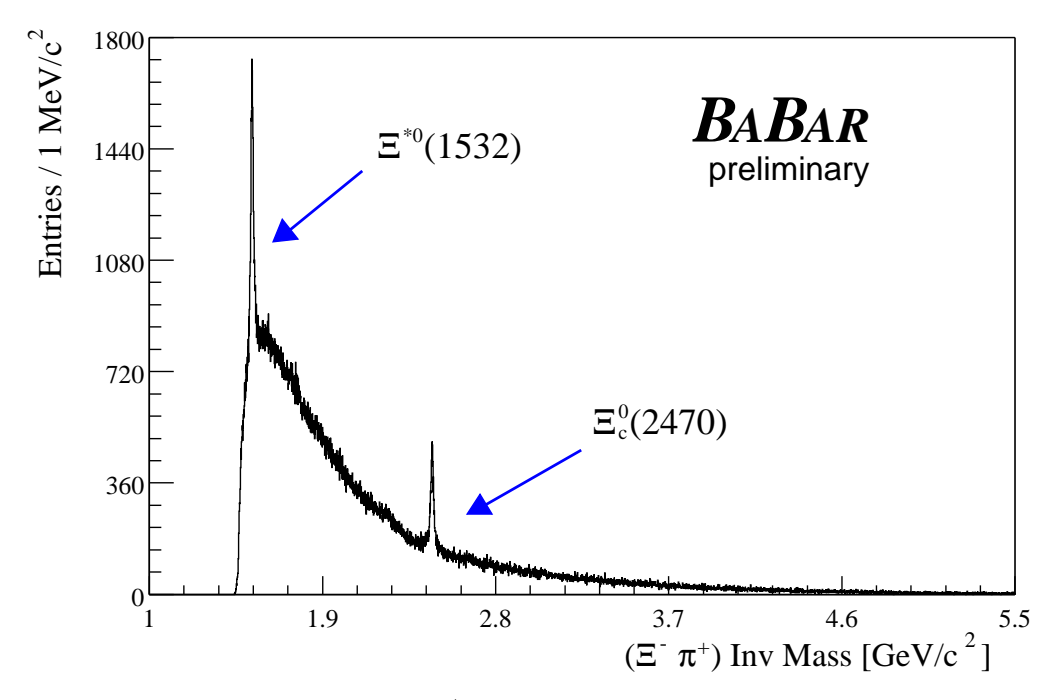


Figure 5: $\Xi^-\pi^+$ invariant mass distribution.

As in the preceding section, we divide the Ξ_5^{--} candidates into ten bins of p^* and find no sign of a pentaquark signal in any bin. We fit a similar signal plus background function to the $\Xi^-\pi^-$ invariant mass distribution in each bin. The resolution function is derived in this case from the $\Xi^{*0}(1530)$ and $\Xi_c^0(2470)$ data and simulation, and is described by a Gaussian with an rms of 8 MeV/ c^2 . For the Breit-Wigner width we consider two possiblities, 1 and 18 MeV/ c^2 , corresponding to a very narrow state and the upper limit on the Ξ_5^{--} width, respectively. The fits are performed over the mass range from 1760 to 1960 MeV/ c^2 , and the background function is a seventh-order polynomial.

Fixing the Ξ_5^{--} mass to 1862 MeV/ c^2 , we obtain the signal yields shown in Fig. 6. In all p^* bins the fit quality is good across the full mass range and the signal is consistent with zero. Systematic uncertainties on the fitting procedure are again found to be negligible compared with the statistical uncertainties, and variations of the Ξ_5^{--} mass and selection criteria give consistent results.

5 Search for $\varXi_5^-,\, \varXi_5^0,\, N_5^0$ and N_5^+ in the \varLambda^0K and \varSigma^0K modes

We search for pentaquark states decaying into a $\Lambda^0 K$ or $\Sigma^0 K$ final state, where K is a charged or neutral kaon, $\Sigma^0 \to \Lambda^0 \gamma$ and $\Lambda^0 \to p\pi^-$. These final states give us access to the Ξ_5^- , Ξ_5^0 , N_5^0 and N_5^+ states (see Fig. 1). The Ξ_5^0 has been reported with a mass of 1862 MeV/ c^2 , and we expect a quite similar mass for the Ξ_5^- ; since our decay modes include two strange particles, we are sensitive only to N_5^0 and N_5^+ states with substantial $s\bar{s}$ content, and these might be expected somewhere between 1500 and 1900 MeV/ c^2 .

We first reconstruct $\Lambda^0 \to p\pi^-$ candidates from all pairs of charged tracks in which one

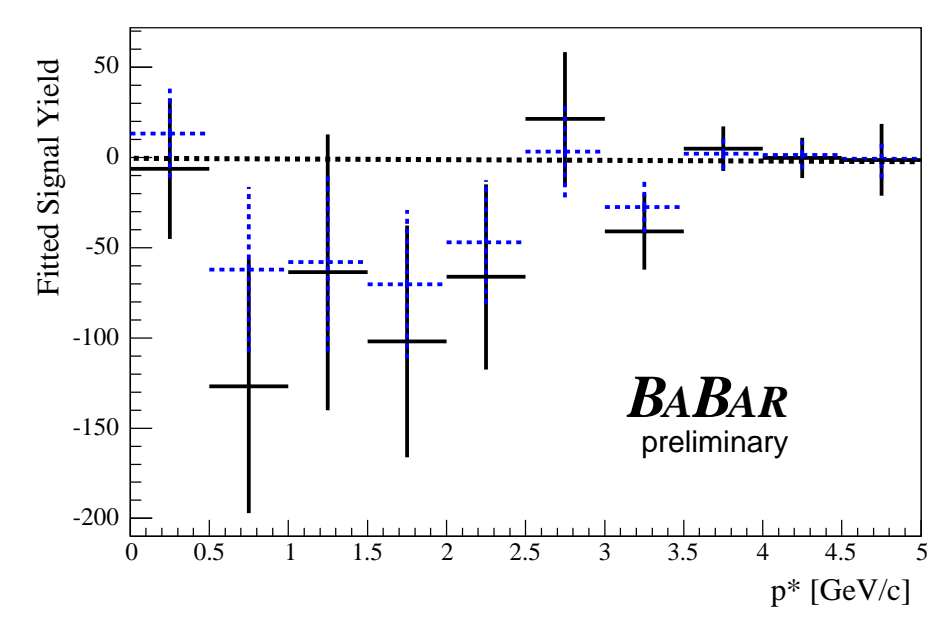


Figure 6: The Ξ_5^{--} signal yields extracted from the fits to the $\Xi^-\pi^-$ invariant mass distributions, assuming a Ξ_5^{--} mass of 1862 MeV/ c^2 and width $\Gamma = 1$ (dashed) and $\Gamma = 18$ MeV/ c^2 (solid).

satisfies tight proton identification requirements, and the other loose pion identification. The pairs are required to form a good vertex, to have an angle between their flight direction (line from the IP to the vertex) and total momentum at the vertex less than 200 mrad, and to have an invariant mass within 20 MeV/ c^2 of the nominal Λ^0 mass. To reconstruct Σ^0 candidates, The Λ^0 candidates are combined with neutral (not associated with any charged track) calorimetric energy deposits of at least 80 MeV that do not pair with any other neutral deposit to form a π^0 candidate. We require a mass difference $M_{p\pi\gamma} - M_{p\pi}$ within 20 MeV/ c^2 of the nominal $M_{\Sigma^0} - M_{\Lambda^0}$ value. Similarly, K_s^0 candidates are reconstructed from pairs of oppositely charged tracks forming a good vertex, having an angle between their flight direction and total momentum less than 30 mrad, and having an invariant mass within 4.5 MeV/ c^2 of the nominal K_s^0 mass. Charged kaon candidates are required to be consistent with coming from the IP and to pass tight kaon identification requirements. The simulated signal reconstruction efficiencies vary from 0.5% for the $\Sigma^0 K_s^0$ mode to 10% for the $\Lambda^0 K^\pm$ modes at low p^* , and increase to 3% and 25%, respectively, at high p^* .

We find a substantial p^* dependence in the structure of the invariant mass distributions, and so we show them in four p^* bins, for $\Lambda^0 K^+$, $\Lambda^0 K^-$ and $\Lambda^0 K^0_s$ combinations in Figs. 7, 8 and 9, respectively, and for $\Sigma^0 K^+$, $\Sigma^0 K^-$ and $\Sigma^0 K^0_s$ combinations in Figs. 10, 11 and 12, respectively. In Fig. 7 there is a peak as expected from $\Lambda_c^+(2285)$ and also some structure in the 1950–2150 MeV/ c^2 region that can be attributed to Λ_c^+ decays with one or two missing pions. No other narrow peaks are evident.

In Fig. 8 the Ω^- peak is prominent and there is a hint of a broad structure corresponding to the $\Xi^-(1820)$, but no other narrow structure is visible. In Fig. 9 we observe the $\Xi_c^0(2472)$ at high momenta, and there are hints of the $\Xi^0(1820)$, but no other narrow structure. The $\Sigma^0 K$ modes have much lower statistics, but show structure consistent with the corresponding

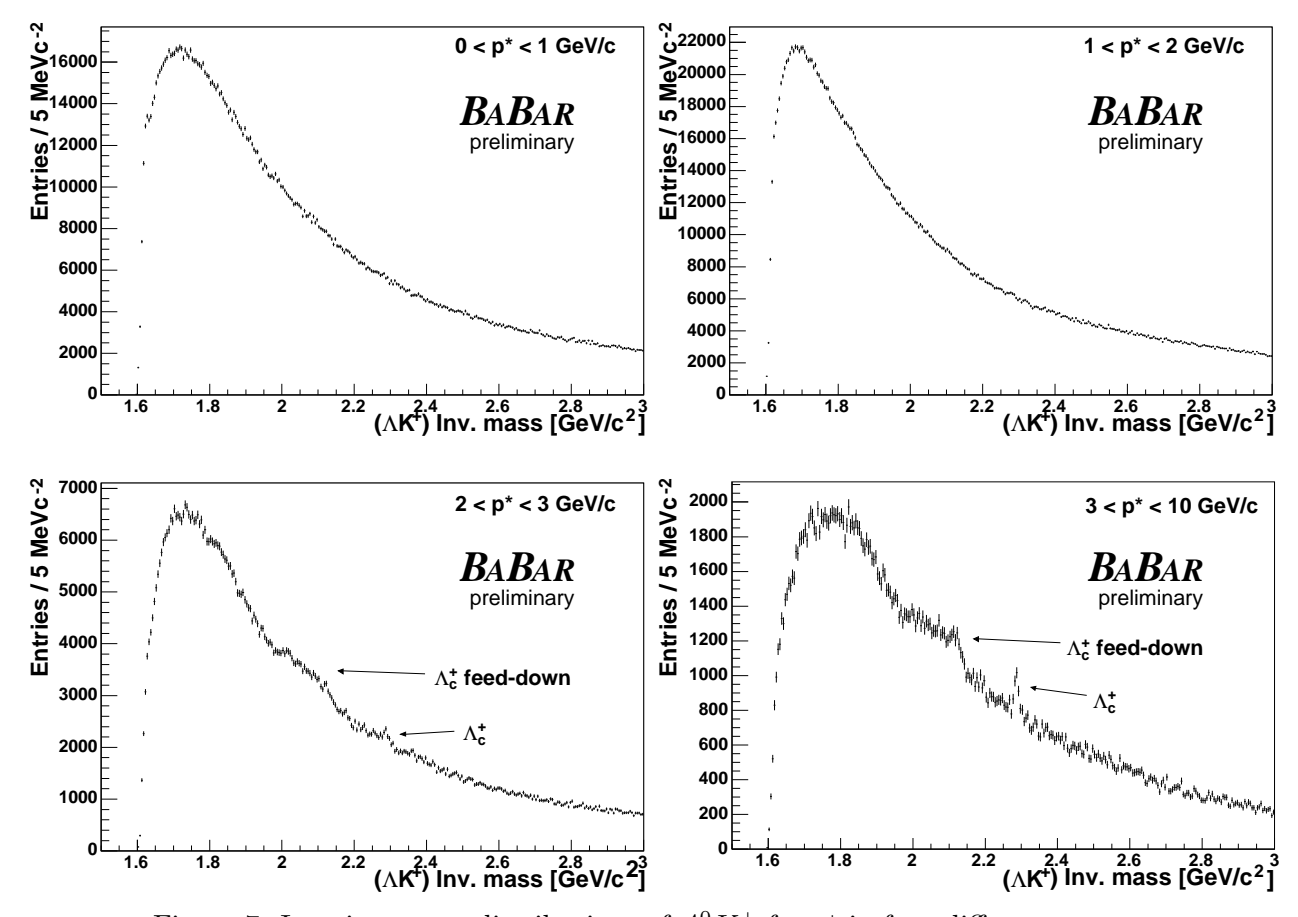


Figure 7: Invariant mass distributions of $\Lambda^0 K^+$ for p^* in four different ranges.

 $\Lambda^0 K$ mode. There is a hint of the $\Xi^-(1950)$ at low p^* in the $\Sigma^0 K^-$ mode. In no case is any unexpected narrow structure seen, and all evident structure is consistent with that due to known resonances. We have also examined the data in finer p^* bins and find no sign of a pentaquark signal in any p^* range.

We perform fits in ten p^* bins to the $\Lambda^0 K^-$ and $\Lambda^0 K^0_s$ mass distributions, in which we might expect signals near 1860 MeV/ c^2 from the Ξ_5^- and Ξ_5^0 states, respectively. The resolution functions derived from the data and simulation are described by sums of two Gaussians with total rms of about 4 MeV/ c^2 that depend slightly on p^* . For each Breit-Wigner width we consider both 1 and 18 MeV/ c^2 , as for the Ξ_5^{--} . The fits are performed over the mass range from 1772 MeV/ c^2 to 1972 MeV/ c^2 in order to exclude known resonances. The background function is a first-order polynomial.

We fix the masses to $1862 \text{ MeV}/c^2$, plus a shift obtained from the simulation in each p^* bin that does not exceed $2 \text{ MeV}/c^2$, and obtain the signal yields shown in Fig. 13. In all p^* bins the fit quality is good across the full mass range and the signal is consistent with zero. Systematic uncertainties on the fitting procedure are again found to be negligible compared with the statistical uncertainties, and variations of the mass and selection criteria give consistent results.

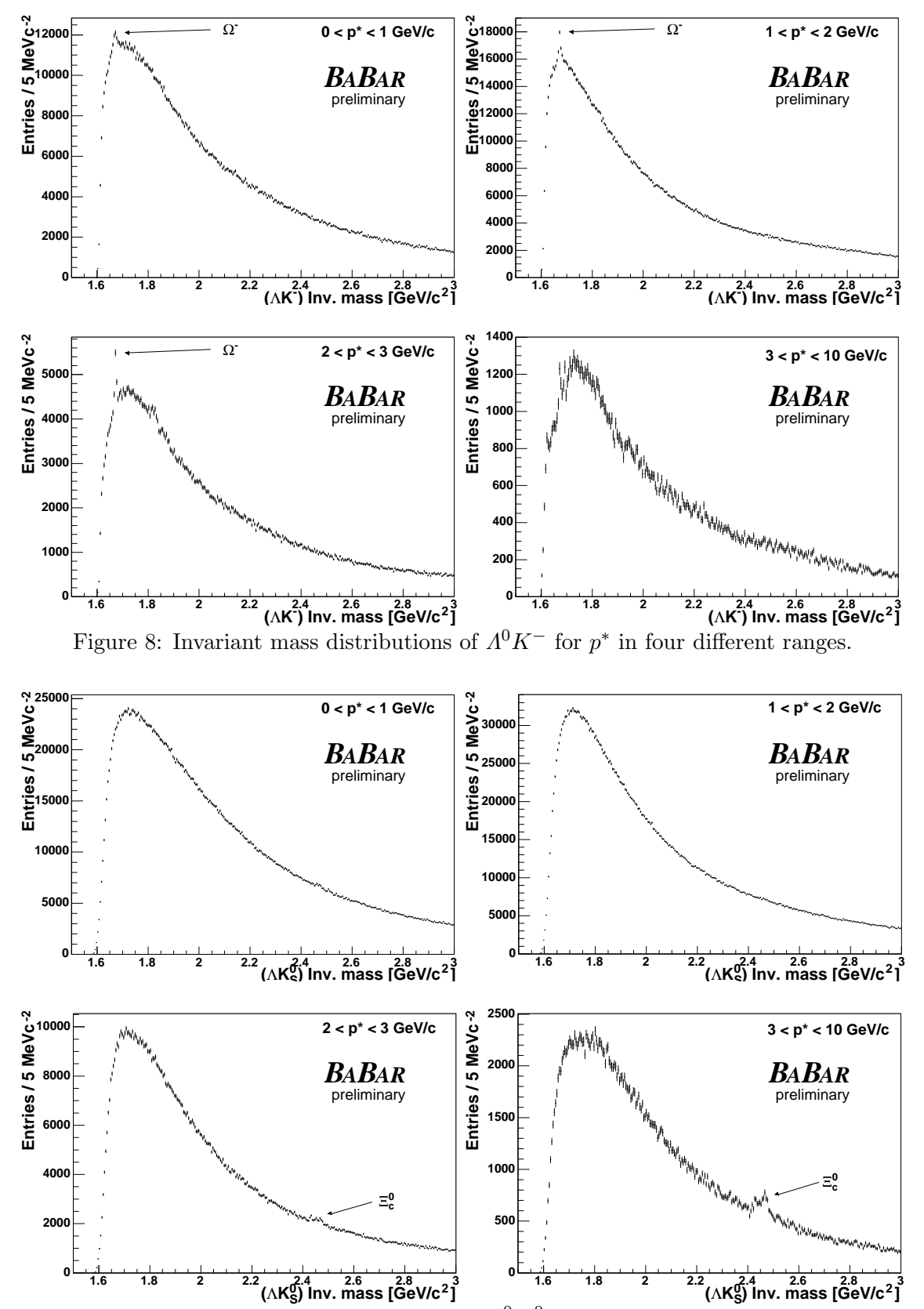


Figure 9: Invariant mass distributions of $\Lambda^0 K_S^0$ for p^* in four different ranges.

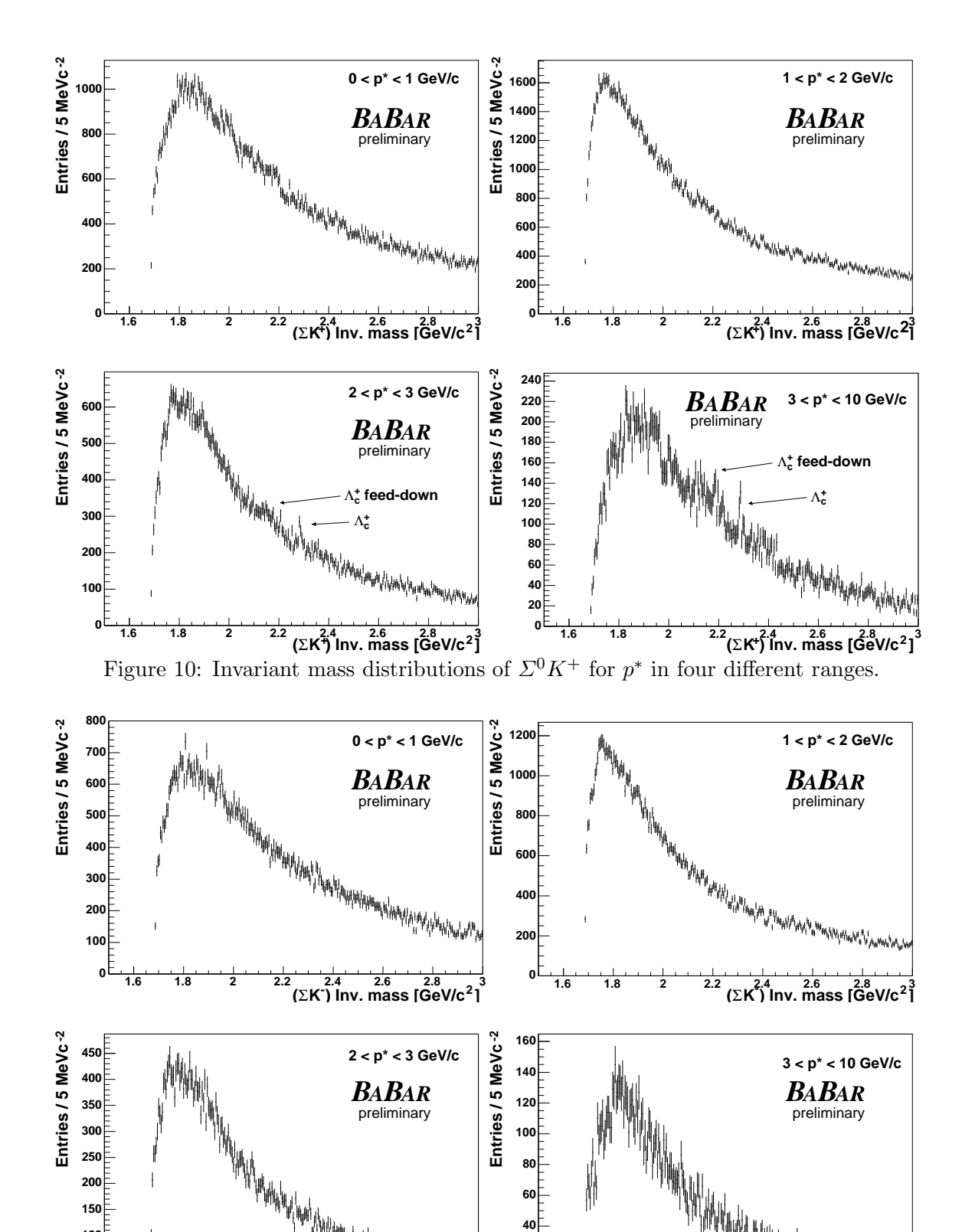


Figure 11: Invariant mass distributions of $\Sigma^0 K^-$ for p^* in four different ranges.

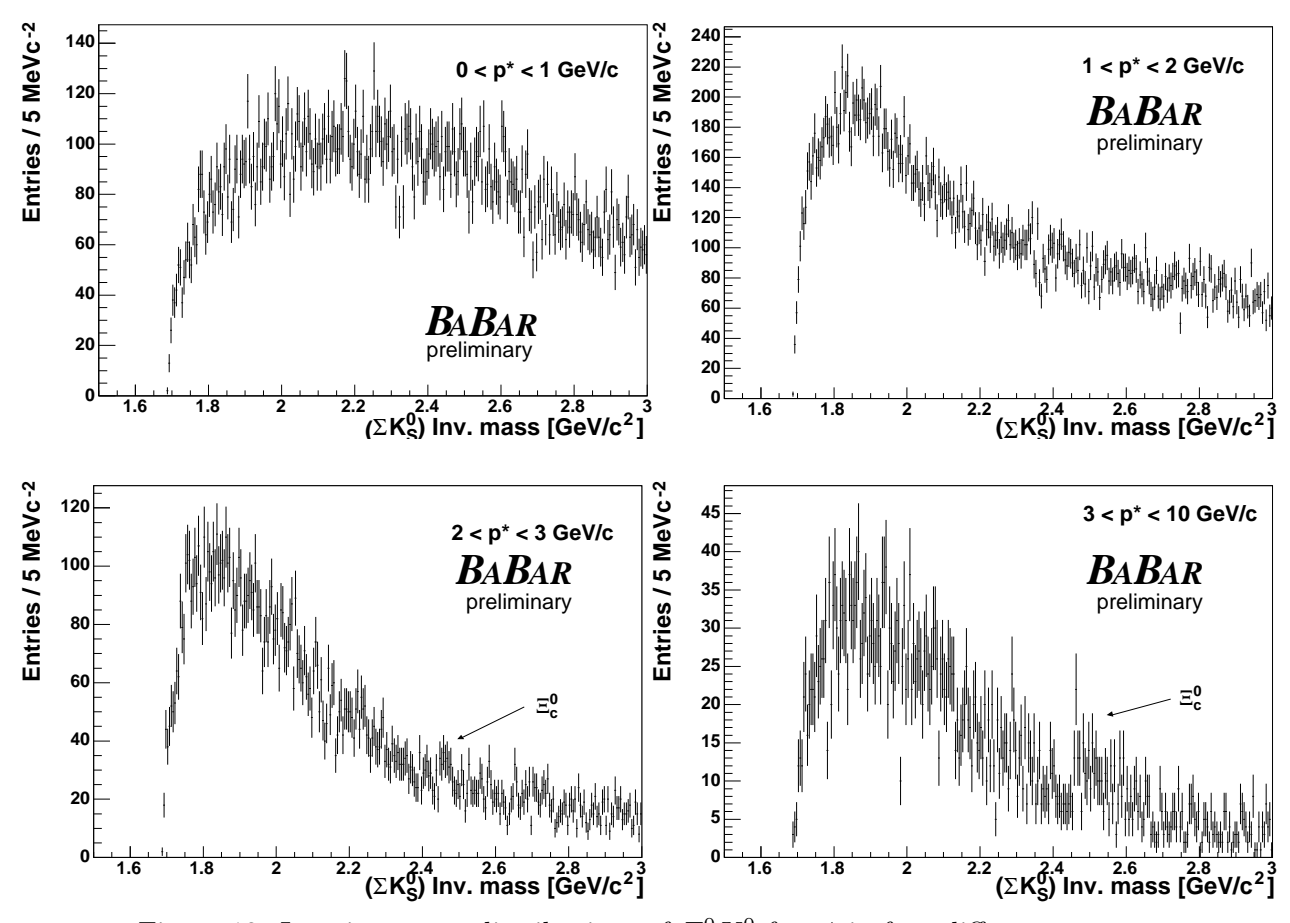


Figure 12: Invariant mass distributions of $\Sigma^0 K_S^0$ for p^* in four different ranges.

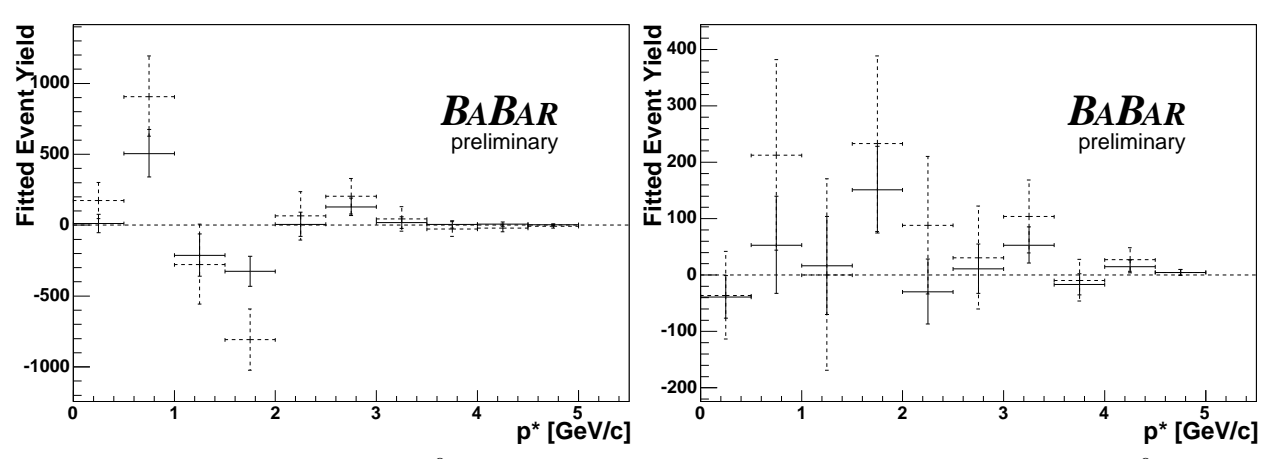


Figure 13: The Ξ_5^- (left) and Ξ_5^0 (right) signal yields extracted from the fits to the $\Lambda^0 K^-$ and $\Lambda^0 K_S^0$ mass distributions, respectively, assuming a mass of 1862 MeV/ c^2 and width $\Gamma=1$ (solid) and $\Gamma=18$ MeV/ c^2 (dashed).

6 Upper Limits

For the states reported by previous experiments, there exist specific masses at which to search and experimental upper limits on the decay widths. We can therefore calculate upper limits on their differential production cross sections, with some assumptions on the branching fraction to the mode in which the search was made. We present such limits for the Θ_5^+ , Ξ_5^{--} , Ξ_5^- and Ξ_5^0 .

For the $\Theta_5^+(1540) \to pK_S^0$ we take the yields from the fits shown above (see Fig. 3) and convert them into cross sections by dividing by the efficiency (including the $K_S^0 \to \pi^-\pi^+$ branching fraction), the integrated luminosity and the p^* bin width. The reconstruction efficiency is calculated from the simulation and corrected using data, and varies smoothly from 13% at low p^* to 22% at high p^* . It is checked by measuring the differential cross section for $\Lambda_c^+ \to pK_S^0$ in the combination of $q\bar{q}$ and $\Upsilon(4S)$ events represented in our data, which is found to be consistent with the appropriate combination of previous measurements. If the Θ_5^+ is a $udud\bar{s}$ pentaquark state, we expect only two possible decay modes, nK^+ and pK^0 , with very similar Q values and hence roughly equal branching fractions. Assuming half of the K^0 appear as K_S^0 , we arrive at a branching fraction $B(\Theta_5^+ \to pK_S^0) = 1/4$, and we divide by this value to obtain the total Θ_5^+ differential production cross section.

We then derive a conservative upper limit on this cross section in each bin. We consider only the physically allowed region, and scale the limit by a factor of $(1 + \delta \epsilon/\epsilon)$, where $\delta \epsilon/\epsilon = 0.049$ is the sum in quadrature of the relative systematic uncertainties on the efficiency and luminosity. The relative luminosity uncertainty is 1%, and that on the efficiency is dominated by the 3.2% uncertainty on the reconstruction of pairs of tracks from a displaced vertex such as a K_s^0 . The total is nearly independent of p^* .

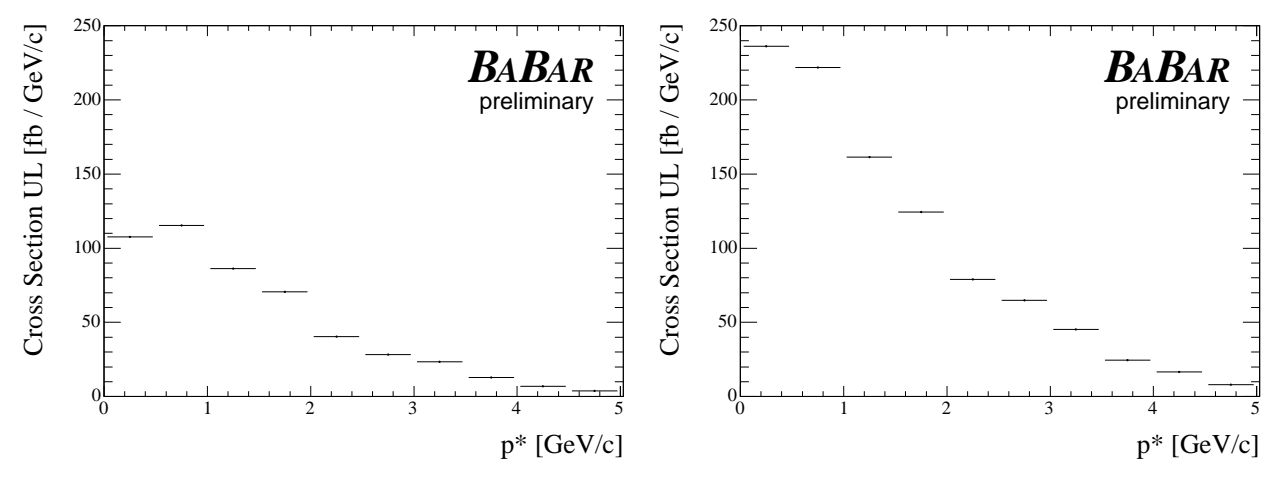


Figure 14: The 95% C.L. upper limit on the production cross-section for the Θ_5^+ assuming a mass of 1540 MeV/ c^2 and a natural width $\Gamma=1$ MeV/ c^2 (left) or $\Gamma=8$ MeV/ c^2 (right), as a function of c.m. momentum p^* .

These upper limits are shown in Fig. 14 and tabulated in Table 2. Two sets of limits are shown; one corresponds to a very narrow state, and the other to a width at the current experimental upper limit of 8 MeV/ c^2 . The limits correspond to the mass of 1540 MeV/ c^2 used in the fits; repeating the analysis at several nearby mass values gives consistent limits.

The units are fb per GeV/c, and apply to the sum of all possible production processes. To isolate continuum and $\Upsilon(4S)$ production we divide by the respective cross sections, and the corresponding limits on the numbers of pentaquarks per event are given in Table 2.

Similarly we convert the measured yields described above for the $\Xi_5^{--}(1862) \to \Xi^-\pi^-$ (Fig. 6), $\Xi_5^-(1862) \to \Lambda^0 K^-$ (Fig. 13) and $\Xi_5^0(1862) \to \Lambda^0 K_S^0$ (Fig. 13) decays into cross sections. Here we assume a mass of $1862 \text{ MeV}/c^2$ and present limits for both a very narrow hypothesis and for $\Gamma = 18 \text{ MeV}/c^2$. The $\Xi_5^{--}(1862) \to \Xi^-\pi^-$ reconstruction efficiency varies smoothly from 6.5% at low p^* to 12% at high p^* , and has been checked using the observed $\Xi^{*0}(1530) \to \Xi^-\pi^+$ signal. Its relative systematic uncertainty again varies slightly with p^* , and its average value of $\delta\epsilon/\epsilon = 0.064$ is larger than for the pK_S^0 mode, as there are two displaced vertices and more tracks in the decay. The $\Xi_5^-(1862) \to \Lambda^0 K^-$ efficiency varies from 10% at low p^* to 27% at high p^* , is checked with the $\Omega^- \to \Lambda^0 K^-$ signal, and the average $\delta\epsilon/\epsilon = 0.052$ is similar to the pK_S^0 mode. The $\Xi_5^0(1862) \to \Lambda^0 K_S^0$ efficiency varies from 3.5% at low p^* to 13% at high p^* , and $\delta\epsilon/\epsilon = 0.072$ is similar to the $\Xi^-\pi^-$ mode.

We assume a $\Xi_5^{--} \to \Xi^-\pi^-$ branching fraction of one-half; for the Ξ_5^- and Ξ_5^0 we do not assume branching fractions into the measured modes, but present limits on the product of the production cross section and branching fraction. Again the results are independent of the assumed mass; they are shown in Figs. 15 and 16, and tabulated in Tables 3, 4 and 5.

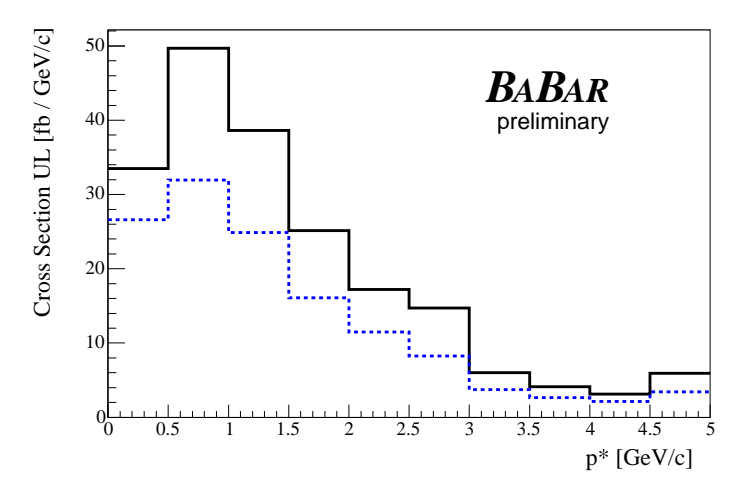


Figure 15: The 95% C.L. upper limit on the production cross-section for Ξ_5^{--} assuming a natural width of $\Gamma = 1$ (dashed) and $\Gamma = 18$ MeV/ c^2 (solid), as a function of c.m. momentum p^* .

In order to quote limits on the total production cross section (times branching fraction) we must either know the momentum spectrum or believe that it does not vary rapidly on the scale of our bin size. Since the latter is true in the simulation, we assign conservative, model-independent upper limits on the total numbers of pentaquarks produced per $e^+e^- \rightarrow q\bar{q}$ event ($\Upsilon(4S)$ decay) by summing each differential cross section over the p^* range from zero to the kinematic limit for 5.3 GeV jets (B meson decays), taking into account the fact that most of the systematic error is common to all bins. Limits are derived from these sums by the same method as in each bin, and are listed in Tables 2–5. Any postulated spectrum can be folded with our differential limit to obtain a limit on the total cross section assuming that spectrum, which will be lower than the model independent limits given in the tables.

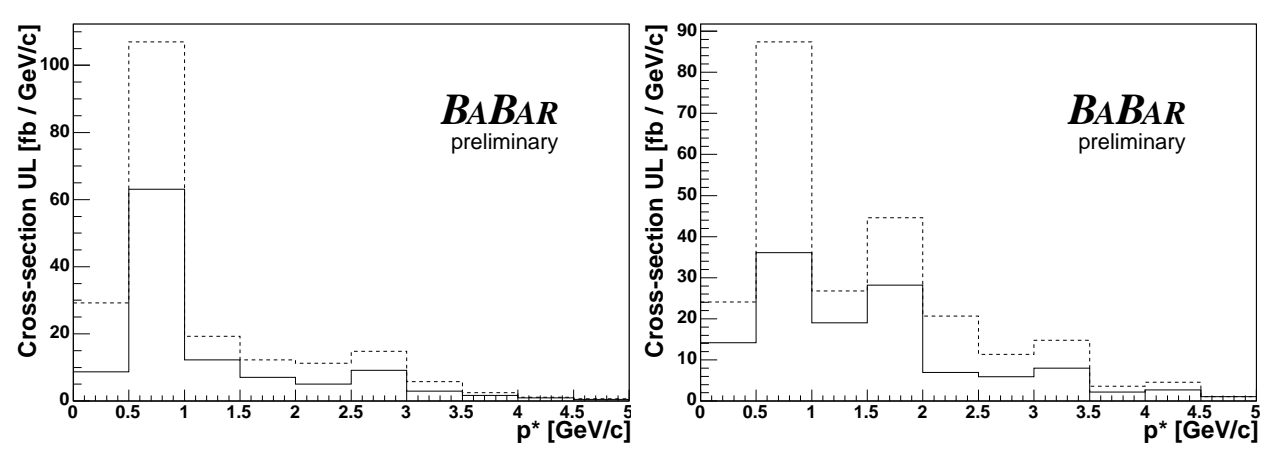


Figure 16: The 95% C.L. upper limits on the production cross-section for Ξ_5^- times its branching fraction into $\Lambda^0 K^-$ (left), and Ξ_5^0 times its branching fraction into $\Lambda^0 K_S^0$ (right), assuming a natural width of $\Gamma = 1$ MeV/ c^2 (solid) and $\Gamma = 18$ MeV/ c^2 (dashed), as a function of c.m. momentum p^* .

7 Summary

We have performed a preliminary high statistics search for the reported states Θ_5^+ (1540), Ξ_5^- (1862), Ξ_5^- (1862) and Ξ_5^0 (1862) in e^+e^- annihilations, and also for most of the other members of the pentaquark octet and anti-decuplet to which they are postulated to belong. In all cases we observe clear signals for known baryon resonances that demonstrate sensitivity to any new narrow resonances, with invariant mass resolution better than the reported upper limits on the widths of the respective states. We find no evidence for the production of such states in 123 fb⁻¹ of *BABAR* data. For the reported states, we see no excess at the measured invariant mass values and use the reported limits on their widths to set upper limits on the their inclusive production in our search modes in both $e^+e^- \to q\bar{q}$ events events and $\Upsilon(4S)$ decays. These limits are at the level of 10^{-4} – 10^{-5} per event, depending on the width assumed, and are valid for any narrow state in the vicinity of 1540 or 1860 MeV/ c^2 . The searches for other members of the multiplets show no evidence for an unknown narrow resonance at any mass between threshold for the decay mode used and the kinematic limit.

In order to limit the production rates we must know the branching fraction of each state into the decay mode used in the search. In the case of the Θ_5^+ , we take this to be 1/4, as noted above. For Ξ_5^{--} a similar argument that $\Xi^-\pi^-$ and Σ^-K^- dominate and have roughly equal branching fractions leads to a branching fraction of 1/2. Taking the upper limit widths, we calculate 95% C.L. upper limits on the total production rates of 1.1×10^{-4} Θ_5^+ and 1.0×10^{-5} Ξ_5^{--} per $e^+e^- \to q\bar{q}$ event (preliminary); these are roughly a factor of eight and four below the typical values measured for ordinary octet and decuplet baryons of the same masses of 8×10^{-4} and 4×10^{-5} , respectively, as illustrated in Fig. 17.

The situation is more complex for the Ξ_5^- and Ξ_5^0 as the mixing between the members of the anti-decuplet and the octet is unknown. In these two cases the branching fraction of an antidecuplet state of mass $\sim 1860 \text{ MeV}/c^2$ to the measured mode could be anywhere from zero to $\sim 1/3$. The best limit that could be set, assuming the value of 1/3, would therefore be roughly 15×10^{-5} Ξ_5^- or Ξ_5^0 per $e^+e^- \to q\bar{q}$ event, which is well above the "expected" value

Table 2: The measured Θ_5^+ signal yield in each p^* bin, assuming a mass of 1540 MeV/ c^2 and two values of the natural width Γ in MeV/ c^2 . The corresponding upper limits at the 95% C.L. on the Θ_5^+ differential production cross section, the number of Θ_5^+ produced per $e^+e^- \to q\bar{q}$ event and the number per $\Upsilon(4S)$ decay.

	$\Theta_5^+(1540)$ (preliminary)										
p^* Range	Yield		X-section U.L.		$q\bar{q}$ event U.L.		$\Upsilon(4S)$ decay U.L.				
$(\mathrm{GeV}\!/c)$	$(pK_s^0 \text{ mode})$		$({\rm fb/GeVc^{-1}})$		$(10^{-5}/({\rm evt \cdot GeVc^{-1}}))$		$(10^{-5}/(\text{evt}\cdot\text{GeVc}^{-1}))$				
	$\Gamma = 1$	$\Gamma = 8$	$\Gamma = 1 \mid \Gamma = 8$		$\Gamma = 1$	$\Gamma = 8$	$\Gamma = 1$	$\Gamma = 8$			
0.0 – 0.5	$107\pm_{134}^{139}$	$288\pm_{242}^{283}$	107.6	236.2	3.17	6.97	10.76	23.62			
0.5 – 1.0	$-178\pm_{236}^{238}$	$-194\pm^{457}_{452}$	115.3	221.8	3.40	6.54	11.53	22.18			
1.0 – 1.5	$19\pm_{208}^{210}$	$-31\pm_{410}^{406}$	86.2	161.5	2.54	4.76	8.61	16.14			
1.5 – 2.0	$109\pm_{156}^{156}$	$112\pm_{310}^{307}$	70.7	124.4	2.09	3.67	7.07	12.44			
2.0 – 2.5	$-158\pm^{114}_{113}$	$-322\pm_{243}^{222}$	40.4	79.0	1.19	2.33	2.83	7.90			
2.5 – 3.0	$-38\pm {83\atop 83}$	$41\pm_{164}^{175}$	28.3	64.8	0.83	1.91	2.35	6.48			
3.0 – 3.5	$33\pm {}^{59}_{59}$	$50\pm^{119}_{117}$	23.4	45.2	0.69	1.33		_			
3.5 – 4.0	$-11\pm \frac{39}{39}$	$-56\pm {74\atop 80}$	12.9	24.5	0.38	7.23		_			
4.0 – 4.5	$4\pm \frac{22}{21}$	$25\pm {}^{47}_{44}$	6.8	16.6	0.20	4.88		_			
4.5 – 5.0	$1\pm {}^{12}_{12}$	$6\pm \frac{24}{24}$	3.7	7.9	0.11	2.33		_			
Total	_	_	182.8	363.1	5.39	10.71	17.90	34.98			
			(fb)		$(10^{-5}/\text{event})$		$(10^{-5}/\text{event})$				

of 4×10^{-5} . The study of additional modes is needed to elucidate the production properties of these states.

Acknowledgements

We are grateful for the extraordinary contributions of our PEP-II colleagues in achieving the excellent luminosity and machine conditions that have made this work possible. The success of this project also relies critically on the expertise and dedication of the computing organizations that support BABAR. The collaborating institutions wish to thank SLAC for its support and the kind hospitality extended to them. This work is supported by the US Department of Energy and National Science Foundation, the Natural Sciences and Engineering Research Council (Canada), Institute of High Energy Physics (China), the Commissariat à l'Energie Atomique and Institut National de Physique Nucléaire et de Physique des Particules (France), the Bundesministerium für Bildung und Forschung and Deutsche Forschungsgemeinschaft (Germany), the Istituto Nazionale di Fisica Nucleare (Italy), the Foundation for Fundamental Research on Matter (The Netherlands), the Research Council of Norway, the Ministry of Science and Technology of the Russian Federation, and the Particle Physics and Astronomy Research Council (United Kingdom). Individuals have received support from CONACyT (Mexico), the A. P. Sloan Foundation, the Research Corporation, and the Alexander von Humboldt Foundation.

Table 3: The measured \varXi_5^- signal yield in each p^* bin, assuming a mass of 1862 MeV/ c^2 and two values of the natural width in MeV/ c^2 . The corresponding upper limits at the 95% C.L. on the \varXi_5^- differential production cross section, the number of \varXi_5^- produced per $e^+e^- \to q\bar{q}$ event and the number per $\Upsilon(4S)$ decay.

	$\Xi_5^{} \to \Xi^- \pi^- \text{ (preliminary)}$									
p^* Range	Yield		X-section U.L.		$q\bar{q}$ event U.L.		$\Upsilon(4S)$ decay U.L.			
(GeV/c)			$(\mathrm{fb}/\mathrm{GeVc^{-1}})$		$(10^{-5}/(\text{evt}\cdot\text{GeVc}^{-1}))$		$(10^{-5}/(\text{evt}\cdot\text{GeVc}^{-1}))$			
	$\Gamma = 1$	$\Gamma = 18$	$\Gamma = 1$	$\Gamma = 18$	$\Gamma = 1$	$\Gamma = 18$	$\Gamma = 1$	$\Gamma = 18$		
0.0 – 0.5	13 ± 26	-7 ± 37	26.6	33.5	0.78	0.99	2.53	3.19		
0.5 – 1.0	-62 ± 52	-128 ± 67	31.9	49.7	0.94	1.46	3.04	4.73		
1.0 - 1.5	-56 ± 50	-63 ± 76	24.9	38.6	0.73	1.14	2.37	3.68		
1.5 - 2.0	-70 ± 52	-102 ± 62	16.1	25.1	0.47	0.74	1.53	2.39		
2.0 – 2.5	-48 ± 33	8 ± 33 -64 ± 50		17.2	0.34	0.51	1.09	1.64		
2.5 – 3.0	5 ± 28	21 ± 35	8.3	14.7	0.24	0.43	0.79	1.40		
3.0 – 3.5	-25 ± 15	-36 ± 28	3.7	6.0	0.11	0.18	_	_		
3.5 – 4.0	5 ± 10	8±12	2.6	4.1	0.08	0.12	_	_		
4.0 – 4.5	3 ± 10	2 ± 11	2.1	3.1	0.06	0.09	_	_		
4.5 – 5.0	1 ± 12	1±22	3.4	5.9	0.10	0.17		_		
Total	_	_	22.0	33.7	0.65	0.99	2.11	3.20		
			(fb)		$(10^{-5}/\text{event})$		$(10^{-5}/\text{event})$			

Table 4: The measured \varXi_5^- signal yield in each p^* bin, assuming a mass of 1862 MeV/ c^2 and two values of the natural width in MeV/ c^2 . The corresponding upper limits at the 95% C.L. on the \varXi_5^- differential production cross section times its branching fraction B into $\Lambda^0 K^-$, $B\times$ the number of \varXi_5^- produced per $e^+e^-\to q\bar{q}$ event and $B\times$ the number per $\Upsilon(4S)$ decay.

$\Xi_5^- \to \Lambda^0 K^- \text{ (preliminary)}$									
hline p^* Range	Yield		X-section U.L.		$q\bar{q}$ event U.L.		$\Upsilon(4S)$ decay U.L.		
(GeV/c)			$(\mathrm{fb}/\ \mathrm{GeVc^{-1}})$		$(10^{-5}/(\text{evt}\cdot\text{GeVc}^{-1}))$		$(10^{-5}/(\text{evt}\cdot\text{GeVc}^{-1}))$		
	$\Gamma = 1$ $\Gamma = 18$		$\Gamma = 1$	$\Gamma = 18$	$\Gamma = 1$	$\Gamma = 18$	$\Gamma = 1$	$\Gamma = 18$	
0.0 – 0.5	$11\pm {}^{65}_{64}$	$174\pm_{127}^{128}$	40.9	122.4	1.21	3.61	3.90	11.66	
0.5 – 1.0	$505\pm_{164}^{171}$	$906\pm_{277}^{287}$	220.9	385.7	6.52	11.38	21.04	36.73	
1.0 – 1.5	$-213\pm_{148}^{151}$	$-278\pm_{278}^{285}$	62.8	118.8	1.85	3.50	5.98	11.31	
1.5 – 2.0	$-326\pm_{105}^{106}$	$-808\pm_{215}^{216}$	34.3	69.8	1.01	2.06	3.27	6.65	
2.0 – 2.5	$6\pm {85\atop 84}$	$65\pm_{170}^{172}$	24.7	57.2	0.73	1.69	2.35	5.45	
2.5 – 3.0	$129\pm^{62}_{61}$	$203\pm_{125}^{126}$	33.0	59.5	0.97	1.76	_		
3.0 – 3.5	$17\pm {}^{42}_{41}$	$43\pm {}^{87}_{86}$	12.8	27.5	0.38	0.81	_		
3.5 – 4.0	$4\pm \frac{26}{26}$	$-28\pm {}^{53}_{52}$	7.5	13.8	0.22	0.41	_		
4.0 – 4.5	$7\pm {}^{15}_{14}$	$-21\pm \frac{28}{27}$	3.9	6.0	0.12	0.18	_	_	
4.5 – 5.0	$3\pm \frac{6}{5}$	$-8\pm \frac{13}{12}$	1.9	3.3	0.06	0.10			
Total			83.6	181.0	2.76	5.34	7.87	15.88	
			(fb)		$(10^{-5}/\text{event})$		$(10^{-5}/\text{event})$		

Table 5: The measured \varXi_5^0 signal yield in each p^* bin, assuming a mass of 1862 MeV/ c^2 and two values of the natural width in MeV/ c^2 . The corresponding upper limits at the 95% C.L. on the \varXi_5^0 differential production cross section times its branching fraction B into $\Lambda^0 K_S^0$, $B \times$ the number of \varXi_5^0 produced per $e^+e^- \to q\bar{q}$ event and $B \times$ the number per $\Upsilon(4S)$ decay.

$\varXi_5^0 o \varLambda^0 K^0_{\scriptscriptstyle S} \; ext{(preliminary)}$										
p^* Range	Yield		X-section U.L.		$q\bar{q}$ event U.L.		$\Upsilon(4S)$ decay U.L.			
(GeV/c)			$({\rm fb/GeVc^{-1}})$		$(10^{-5}/({\rm evt \cdot GeVc^{-1}}))$		$(10^{-5}/(\text{evt}\cdot\text{GeVc}^{-1}))$			
	$\Gamma = 1$	$\Gamma = 18$	$\Gamma = 1$	$\Gamma = 1 \mid \Gamma = 18$		$\Gamma = 18$	$\Gamma = 1$	$\Gamma = 18$		
0.0 – 0.5	$-39\pm_{38}^{38}$	$-36\pm {}^{78}_{77}$	46.7	95.8	1.38	2.83	4.45	9.12		
0.5 – 1.0	$53\pm_{85}^{87}$	$212\pm_{168}^{169}$	105.7	256.4	3.12	7.56	10.07	24.42		
1.0-1.5	$17\pm_{87}^{87}$	$0\pm_{169}^{171}$	60.6	108.5	1.79	3.20	5.77	10.34		
1.5 – 2.0	$151\pm_{76}^{78}$	$233\pm_{156}^{155}$	71.0	126.2	2.09	3.72	6.76	12.02		
2.0 – 2.5	$-30\pm_{57}^{58}$	$88\pm_{122}^{122}$	23.0	65.3	0.68	1.93	2.19	6.22		
2.5 – 3.0	$11\pm_{43}^{44}$	$31\pm {}^{92}_{91}$	18.1	39.1	0.54	1.15	_	_		
3.0 – 3.5	$53\pm_{32}^{32}$	$104\pm {65\atop 64}$	20.3	40.2	0.60	1.19	_	_		
3.5 – 4.0	$-17\pm_{19}^{19}$	$-9\pm \frac{37}{36}$	6.8	13.2	0.20	0.39				
4.0 – 4.5	$15\pm_{11}^{12}$	$27\pm \frac{21}{21}$	6.9	12.6	0.20	0.37	_	_		
4.5 – 5.0	$5\pm {}^{6}_{5}$	$5\pm {6 \atop 5}$	2.7	2.7	0.08	0.08	_	_		
Total		_	82.8	204.7	2.44	6.04	7.25	18.02		
			(fb)		$(10^{-5}/\text{event})$		$(10^{-5}/\text{event})$			

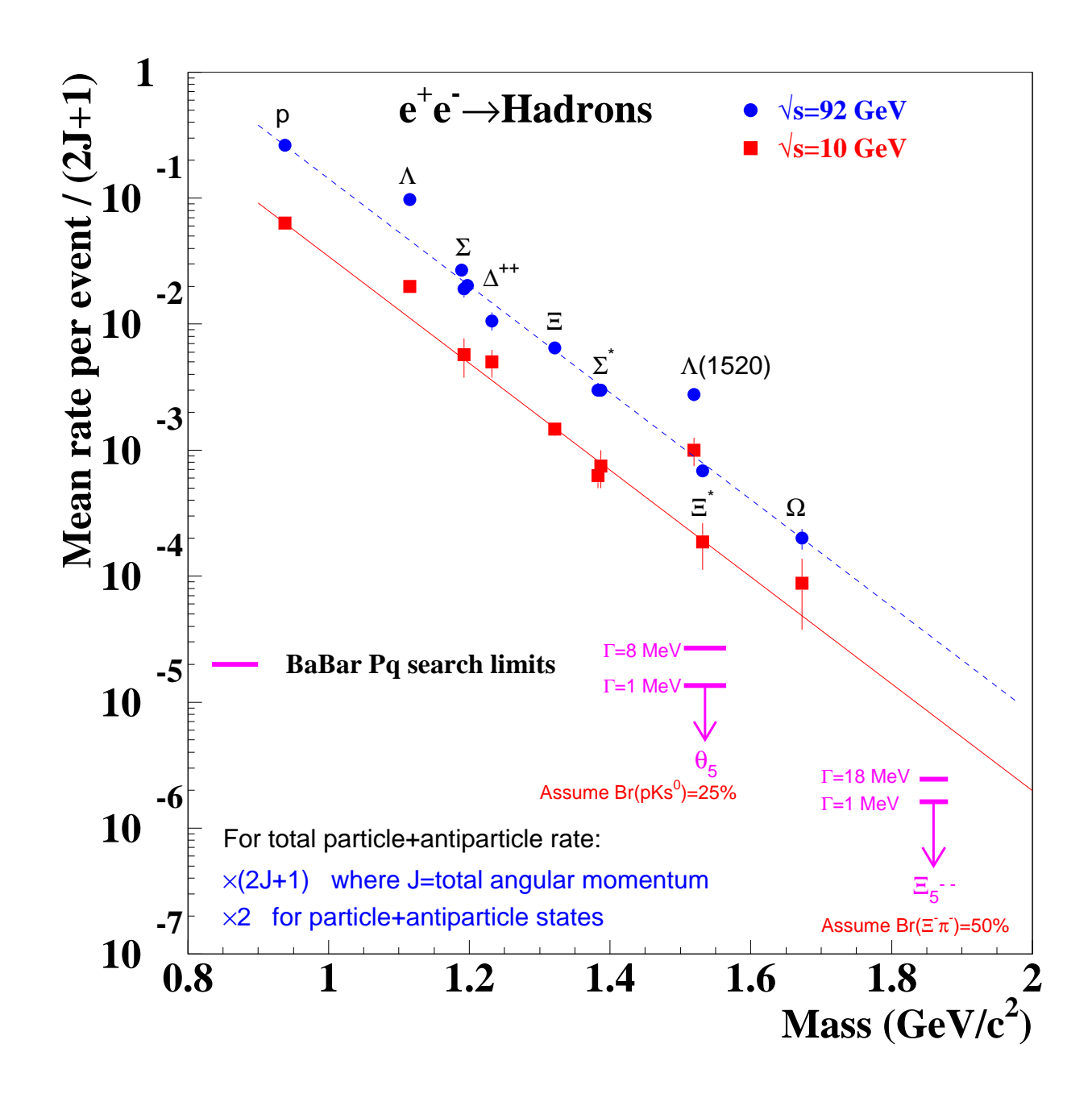


Figure 17: Compilation of baryon production rates in e^+e^- annihilation [15] from experiments at the Z^0 (circles) and $\sqrt{s}\approx 10$ GeV (squares) as a function of baryon mass. The vertical scale accounts for the number of spin and particle+antiparticle states, and the lines are chosen to guide the eye. The arrows indicate our preliminary upper limits on spin-1/2 Θ_5^+ and Ξ_5^{--} pentaquark states, assuming the branching fractions shown, and are seen to lie below the solid line.

References

- [1] LEPS Collaboration, T. Nakano et al., Phys. Rev. Lett. **91**, 012002 (2003).
- [2] SAPHIR Collaboration, J. Barth et al., Phys. Lett. B 572, 127 (2003).
- [3] CLAS Collaboration, V. Kubarovsky *et al.*, Phys. Rev. Lett. **92**, 032001 (2004). Erratum; ibid, 049902.
- [4] DIANA Collaboration, V.V. Barmin et al., Phys. Atom. Nucl. 66, 1715 (2003).
- [5] SVD Collaboration, A. Aleev *et al.*, hep-ex/0401024 (2004).
- [6] HERMES Collaboration, A. Airapetian et al., Phys. Lett. B 585, 213 (2004).
- [7] COSY-TOF Collaboration, M. Abdel-Bary et al., Phys. Lett. B 595, 127 (2004).
- [8] NA49 Collaboration, C. Alt et al., Phys. Rev. Lett. 92, 042003 (2004).
- [9] H1 Collaboration, A. Aktas *et al.*, hep-ex/0403017 (2004).
- [10] See, e.g., J. Pochodzalla, hep-ex/0406077 (2004) and references therein.
- [11] D. Diakonov, V. Petrov and M.V. Polyakov, Z. Phys. A 359, 305 (1997).
- [12] M. Karliner and H. Lipkin, hep-ph/0402260 (2004).
- [13] R. Jaffe and F. Wilczek, Phys. Rev. Lett. **91**, 232003 (2003).
- [14] The BABAR Collaboration, B. Aubert et al., Nucl. Instrum. Methods A 479, 1 (2002).
- [15] Particle Data Group, K. Hagiwara et al., Phys. Rev. **D** 66, 010001 (2002).
- [16] T. Sjostrand, Comput. Phys. Commun. 82, 74 (1994).